LAWRENCE, LYLE, M.S. Ligand Binding to G Protein-Coupled Receptors (GPCRs): 1. 1,8-Naphthyridine Analogs Binding to the Cannabinoid CB2 Receptor 2. Pharmacophore Model Development for Aminoalkylindole Binding to a Novel GPCR (2014)
Directed by Dr. Patricia H. Reggio. 62 pp

Project 1: 1,8-Naphthyridine Analog Binding Model

G-protein coupled receptors (GPCRs) are transmembrane receptors found in eukaryotes that control many cellular signaling events. The cannabinoid receptors, CB1 and CB2, are both GPCRs. These are the receptors that are activated by Δ^9-THC, the principal psychoactive compound in marijuana. CB1 is found mainly in neuronal cells and its activation is thought to lead to the negative, psychoactive side effects of marijuana. CB2 is found in immune cells and in small concentrations in brain tissue. Beneficial effects of activating the cannabinoid receptors include reduction in intraocular pressure, analgesia, antiemesis, and effects on bone density. Designing a drug that can selectively activate CB2, without activating CB1 should lead to analgesia without the negative side effects of CB1. Recent studies have shown the potential of CB2 in treating neurodegenerative diseases such as Parkinson's and Alzheimer's; increasing the importance for developing CB2 selective drugs. Analogs were developed using the 1,8-naphthyridine scaffold that are selective for CB2. These analogs had different activities at CB2 based on their structures. One goal of my thesis project was to develop a model for the binding of 1,8-naphthyridine analogs binding at CB2 and to develop a hypothesis concerning the structural requirements for their production of agonism or antagonism at CB2. The analogs were synthesized and tested by our collaborator, Dr. Clementina Manera at the University of Pisa. Computational modeling techniques were used to

generate conformations of the 1,8-naphthyridine compounds. An automated docking program, Glide, was used to generate the ligand-receptor complexes. The model showed that the presence of a substituent at the C-6 position of the 1,8-naphthyridine ring prevents CB2 from adopting an activated state.

Project 2: Aminoalkylindole Pharmacophore Model

A second goal of my thesis was to develop a pharmacophore model for the newly discovered aminoalkylindole (AAI) receptor. WIN 55212-2 is the prototypical aminoalkylindole (AAI) and is known to act as an agonist at both CB1 and CB2. Recently, our collaborator, Dr. Nephi Stella (University of Washington) discovered that WIN 55212-2 and other AAI compounds bind to a non-CB GPCR found in HEK 293 and T98G cells. AAI analogs were developed to generate a structure activity relationship (SAR). These analogs and their binding data were used to generate a pharmacophore model that explains how these AAI compounds are binding to this new receptor. A pharmacophore model is a set of chemical features and their spatial arrangement that explains how a set of compounds bind to a protein. Computational modeling techniques were used to generate conformations of the AAI compounds. The pharmacophore model was developed in PHASE (Schrodinger, Inc.) using a conformational approach on a set of active compounds. The pharmacophore model shows the importance of four aromatic features, a hydrogen bond acceptor feature, and a hydrophobic feature corresponding to the C-2 position of the indole ring.

LIGAND BINDING TO G PROTEIN-COUPLED RECEPTORS (GPCRS): 1. 1,8-NAPHTHYRIDINE ANALOGS BINDING TO THE CANNABINOID CB2 RECEPTOR 2. PHARMACOPHORE MODEL DEVELOPMENT FOR AMINOALKYLINDOLE BINDING TO A NOVEL GPCR

by

Lyle Lawrence

A Thesis Submitted to
the Faculty of The Graduate School at
The University of North Carolina at Greensboro
in Partial Fulfillment
of the Requirements for the Degree
Master of Science

Greensboro
2014

Approved by

_____
Committee Chair

APPROVAL PAGE

This thesis written by Lyle Lawrence has been approved by the following committee of the Faculty of The Graduate School at The University of North Carolina at Greensboro.

Committee Chair _____

Committee Members _____

_____

_____
Date of Acceptance by Committee

_____
Date of Final Oral Examination

TABLE OF CONTENTS

LIST OF TABLES

Page

LIST OF FIGURES

Page

CHAPTER I

INTRODUCTION

The Cannabinoid Receptors

The cannabinoid CB1 and CB2 receptors belong to the Class A (rhodopsin (Rho) family) of G-protein coupled receptors (GPCRs). CB1 was initially cloned from a rat cerebral cortex cDNA library [1]. CB1 was found to be in the brain at multiple locations including, the hippocampus, cerebellum, and substantia nigra [2]. The second cannabinoid receptor sub-type, CB2 was cloned from a human promyelocytic leukemia cell HL60 cDNA library. This receptor was shown to have high density in peripheral tissue. More specifically, CB2 is located on macrophages and several other immune cells [3]. Because CB1 is found mostly in the brain it is thought to mediate the negative, psychoactive effects of cannabinoid ligands. Recent studies have implicated CB2 in neurodegenerative disease states, such as Alzheimer's, Huntington's disease and Parkinson's disease [4]. CB2 has also been shown to be expressed in high levels in cancer cells and CB2 activation induces tumor apoptosis [5]. These developments show the importance of efforts in finding CB2 selective ligands to possibly treat these diseases.

CB1 and CB2 are Class A G-protein coupled receptors (GPCRs) which act via $G_{i/o}$ proteins [6]. Activation of $G_{i/o}$ proteins results in inhibition of adenylyl cyclase,

which ultimately reduces cyclic AMP levels [6]. The classical model of GPCR function states that once the receptor is activated a heterotrimeric (α, β, and γ subunits) G-protein will couple with the receptor. Insertion of the α5 helix of the Gα subunit results in the exchange of GDP for GTP. GTP binding is followed by dissociation of the β and γ subunits from the α subunit, but the β and γ subunits stay together [7]. The β and γ complex and the α subunit cause downstream effects by interacting with other proteins. Once the signaling event has occurred, the receptor needs to be removed from the cell surface so that it does not continue to signal. The cell does this by phosphorylating serine and threonine residues on the C-terminus of the receptor with GPCR kinases (GRKs). The phosphorylated C-terminus can interact with β-arrestin proteins that cause the receptor to be internalized via clathrin coated pits [8]. This internalization stops the receptor from being able to signal.

The crystal structures of Class A GPCR's like rhodopsin [9], β2-adrenergic receptor [10], sphingosine 1- phosphate receptor [11], and the opioid receptors [12, 13] show these types of receptors have four similar structural features. These similar structural features are: seven transmembrane helices, an extracellular N-terminus, an intracellular C-terminus, and extracellular and intracellular loops that connect the helices. Figure 1 shows an image of CB2 in a lipid bilayer with the G_i G-protein inserted.

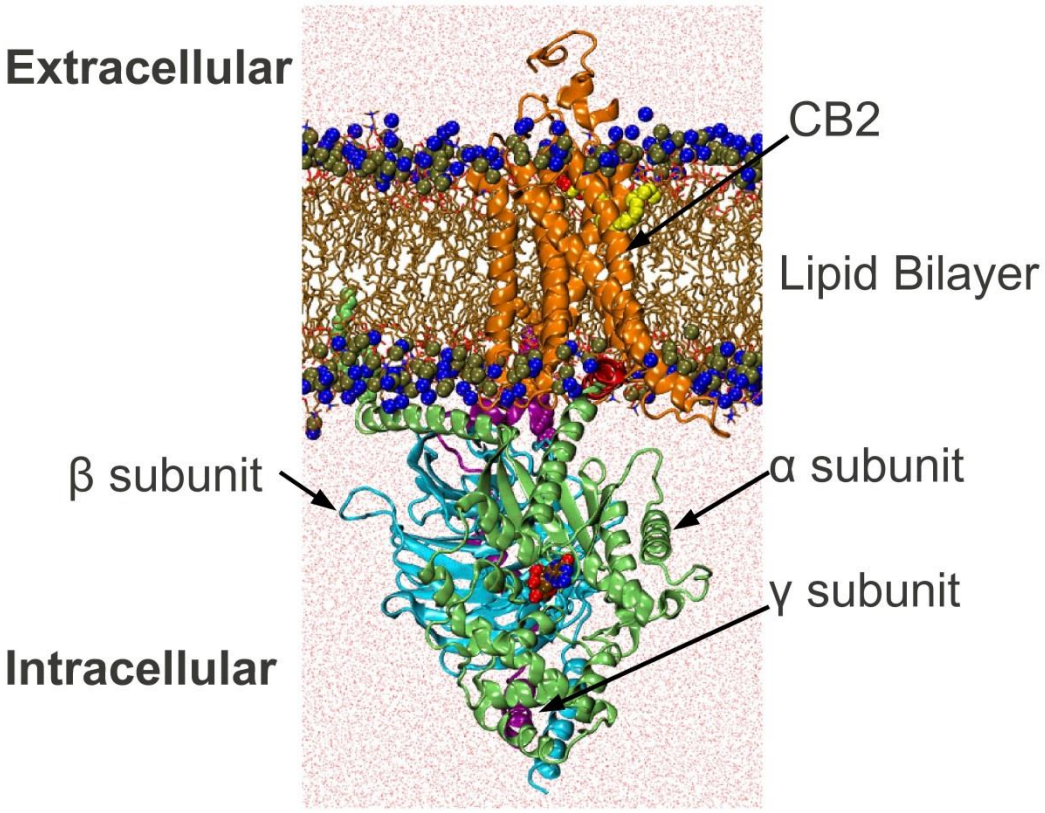

Figure 1. CB2 in Complex with the G_i G-protein in a Lipid Bilayer. CB2 is in orange, heterotrimeric G-protein is in green, cyan, and magenta [14].

CB2 activation requires the completion of several important steps that are similar to many class A GPCRs. In the inactive state of CB2 W6.48 has it's χ1 dihedral in a g+ (-60°) conformation and F3.36 has it's χ1 dihedral in a trans (180°) conformation. W6.48 and F3.36 are important residues known as the "toggle switch" residues. Another pair of important residues are R3.55 and D6.30, these are known as the ionic lock residues. In the inactive state of the receptor R3.55 and D6.30 form a salt bridge with each other to hold the intracellular end of the receptor closed to G-protein insertion. Once activated, the "toggle switch" residues, W6.48 and F3.36 must switch positions. W6.48 undergoes

a χ1 g+ (-60°) → trans (180°) dihedral transition and F3.36 undergoes a χ1 trans (180°) → g+ (-60°) dihedral transition. Figure 2 shows the positions of W6.48 and F3.36 in inactive and active states of CB2. These transitions induce a conformational change in the CWXP flexible hinge region of transmembrane helix 6 (TMH6) that causes TMH6 to straighten and move its intracellular end away for the TMH bundle. The movement of the intracellular end of TMH 6 away from the bundle causes the salt bridge between the ionic lock residues R3.55 and D6.30 to break [15], allowing the intracellular side of the receptor to open for G-protein insertion. Figure 3 shows the distance between TMH3 and TMH6 upon activation of CB2. A ligand that is able to block the transition of W6.48 from g+ to trans would ultimately block the G-protein from coupling. Such a ligand would be considered an antagonist.

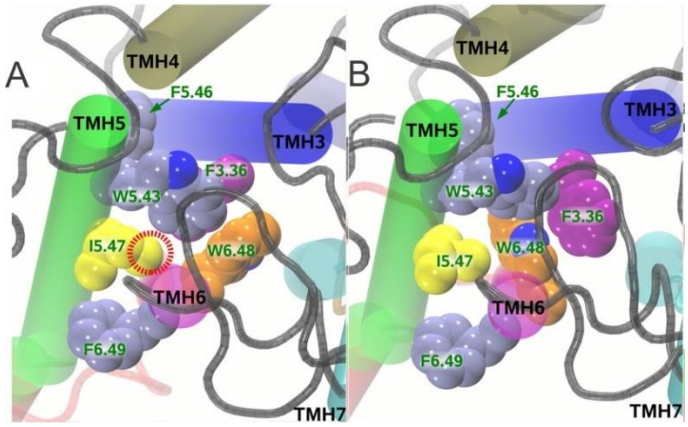

Figure 2. A) Toggle Switch Residues in Inactive State of CB2. W6.48 χ1 in g+ and F3.36 χ1 in trans. B) Toggle Switch Residues in Active State of CB2. W6.48 χ1 in trans and F3.36 χ1 in g+. [15]. W6.48 is shown in orange and F3.36 is shown in magenta.

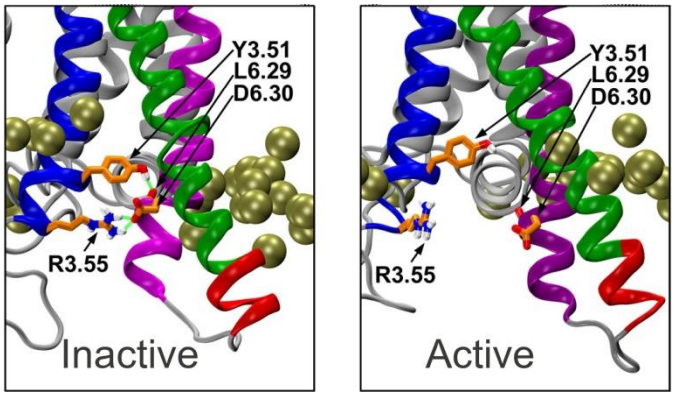

Figure 3. Ionic Lock Residues in Inactive and Active State of CB2. In the active state R3.55 and D6.30 form a salt bridge. In the active state R3.55 and D6.30 are too far apart to form a salt bridge. [15].

Cannabinoid Ligands

Cannabinoid agonists are grouped into four different classes: classical, non-classical, aminoalkylindole, and eicosanoid. The classical group is composed of compounds similar to Δ^9-THC (**1**, Ki CB1=5.05 nM and Ki CB2=80.3 nM), which are dibenzopyran derivatives. A high affinity ligand from this class is HU-210 (**2**), which has higher affinity for CB1 and CB2 than Δ^9-THC (Ki CB1 0.06 nM and Ki CB2 0.17 nM). The non-classical group has compounds that are Δ^9-THC analogs, but lack the pyran ring. The prototype from this group is CP-55940 (**3**), which was developed by Pfizer in 1974 [16] (Ki CB1 0.5 nM and Ki CB2 0.69 nM). The aminoalkylindoles are structurally dissimilar to the classical and non-classical group, having an indole ring with different substituents at N-1 and C-2 positions. The prototypical aminoalkylindole is (R+) WIN 55212-2 (**4**, Ki CB1 1.89 nM and Ki CB2 0.28 nM). The eicosanoids are best exemplified by the two fatty acid derived, endogenous ligands anandamide (**5**, AEA) (Ki CB1 61 nM and Ki CB2 279 nM) discovered in 1992 [17] and 2-arachidonylglycerol (**6**,

2-AG) (Ki CB1 58.3 nM and Ki CB2 145 nM) discovered in 1995 [18]. CB1 and CB2 Ki values taken from Pertwee et al. 2010 review [19]. The compound ajulemic acid (AJA), a synthetic analog of a THC metabolite, Δ^9-THC -11-oic acid, provided an agonist that was selective for CB2 over CB1 and that produced anti-inflammatory, analgesic, and antitumor effects[20, 21]. This showed the potential benefit of creating ligands that can selectively activate CB2 over CB1.

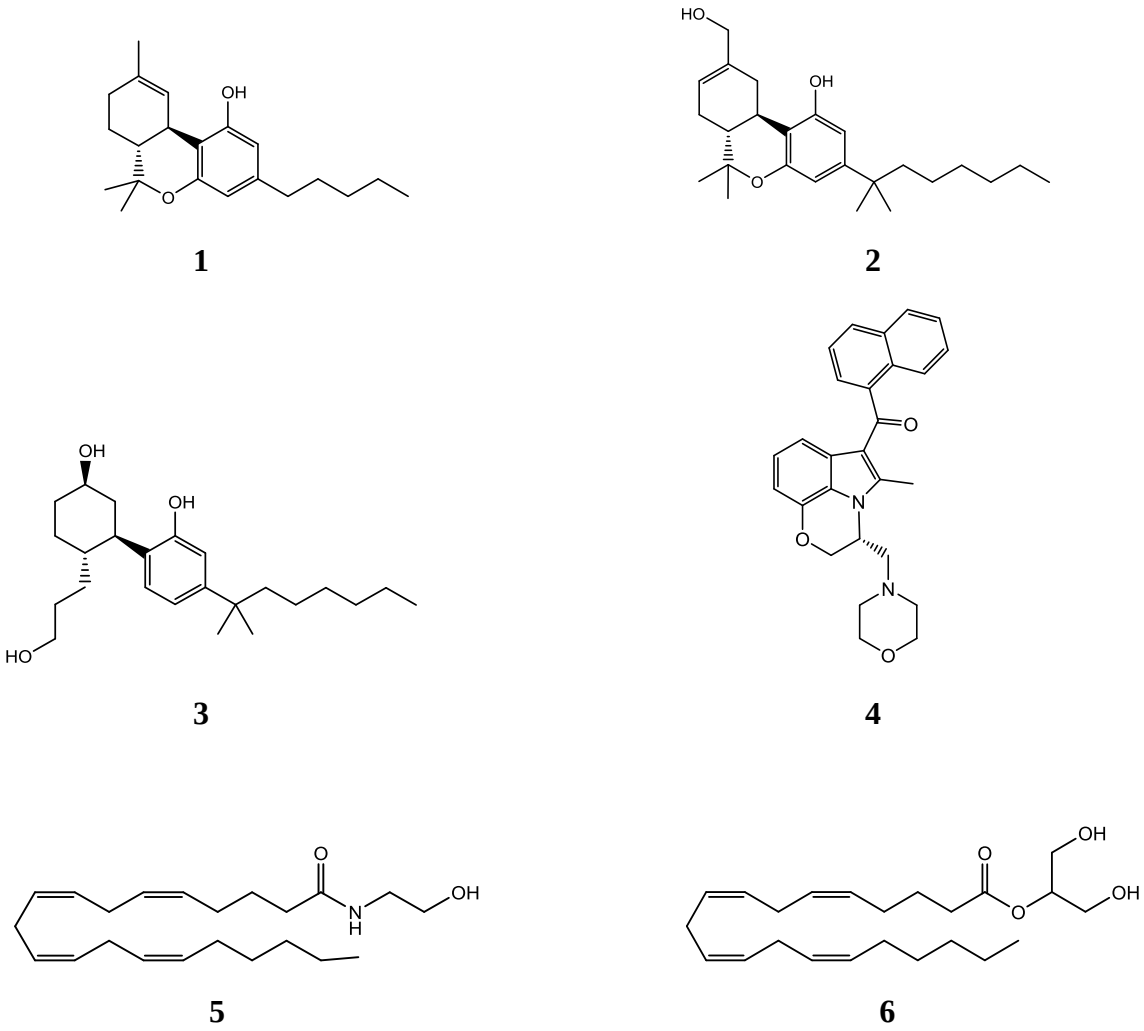

Figure 4. Chemical Structures of Cannabinoid Receptor Agonists.

Two important selective antagonists were developed in the 1990s. SR141716A (**7**) was developed in 1994 as a CB1 selective antagonist (Ki CB1 1.8 nM and Ki CB2 514 nM). SR144528 (**8**) was developed in 1998 as a selective CB2 antagonist (Ki CB1 500 nM and Ki CB2 0.28 nM). These selective antagonists helped distinguish the roles of CB1 and CB2 and which compounds were active at which receptor sub-type. Subsequently, JTE-907 (**9**, Ki CB1 2370 nM and Ki CB2 35.9 nm), a selective CB2 antagonist was developed. JTE-907 contains a quinoline central ring with an amide group at position 3, similar to the SR compounds [22]. The structure of JTE-907 has inspired analogs with a 1,8 naphthyridine ring instead of an quinoline ring. Such 1,8 naphthyridine analogs are a topic in this thesis.

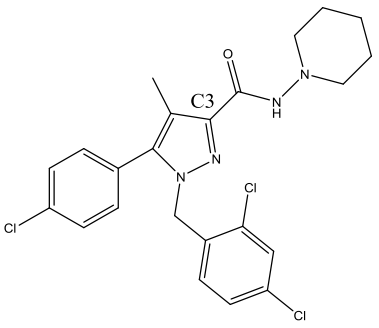

7

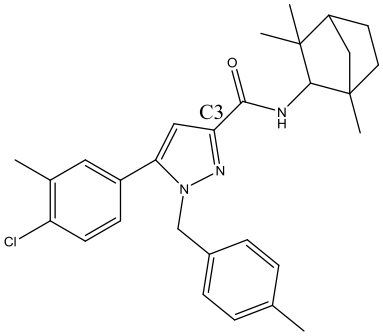

8

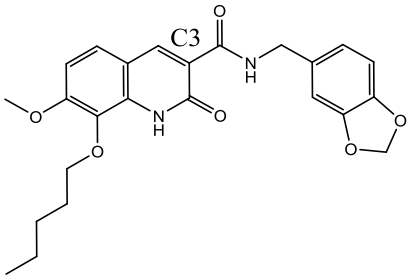

9

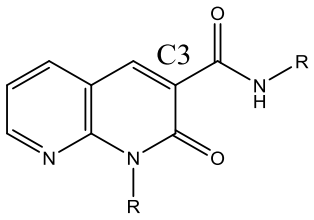

1,8-Naphthyridine Scaffold

Figure 5. Chemical Structures of Cannabinoid Receptor Antagonists and 1,8-Naphthyridine Scaffold.

Project 1: 1,8-Naphthyridine Binding Data

In a collaborative project with the Reggio Lab, Dr. Clementina Manera's group recently produced SAR data for analogs from the 1,8-naphthyridin-2(1*H*)-on-carboxamide scaffold binding to CB2 (unpublished). The goal of this project was to produce CB2 selective ligands from the 1,8-naphthyridine scaffold. Over 20 compounds were synthesized to test the significance of substituents at positions N-1 and C-6 on the naphthyridine ring. Seven CB2 selective compounds (**A1**, **A2**, **5**, **17**, **20**, **21**, and **26**) were tested for their ability to recruit β-arrestin and change cAMP levels. These seven compounds are shown in Figure 6. β-arrestin 2 assays showed of the seven compounds tested that four were agonists and three were antagonists/inverse agonists. WIN55212-2, a CB2 agonist, and SR144528, a CB2 antagonist were used as reference ligands. It was seen that compounds **A1**, **A2**, **5** and **17** were able to recruit β-arrestin 2 in the same manner as WIN55212-2, thus assigning them as agonists. Compounds **20**, **21**, and **26** were able to block β-arrestin 2 recruitment in the same manner as SR144528, thus assigning them as antagonists/inverse agonists. Some assays were inconclusive because compounds **5**, **20**, and **26** were insoluble under the test conditions. For compounds **A1**, **A2**, and **17** it was seen that cAMP levels decrease in a dose dependent manner, which is consistent with agonist activity. Compound **21** was shown to inhibit WIN55212-2 in a dose dependent manner, which is consistent with antagonist activity. The ligands with substituents at position C-6 were seen to be antagonists/inverse agonists. Table 3 in Appendix 2 shows the compounds used to develop the binding model along with CB2 binding affinities and activity data.

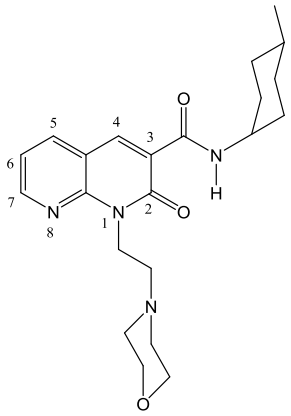

A1

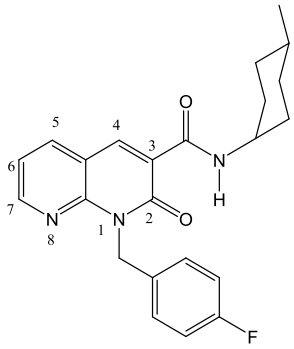

A2

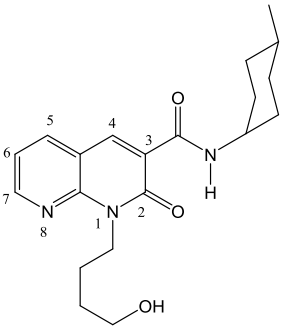

5

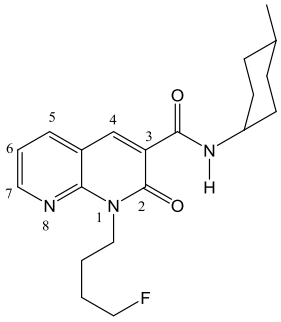

17

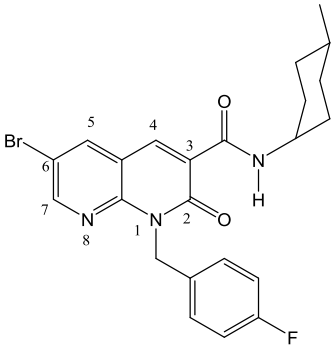

20

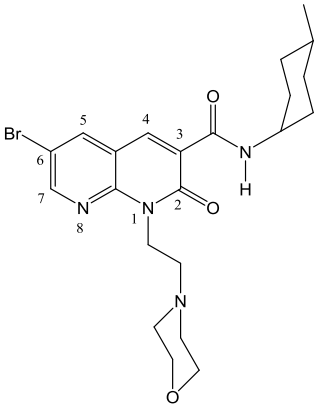

21

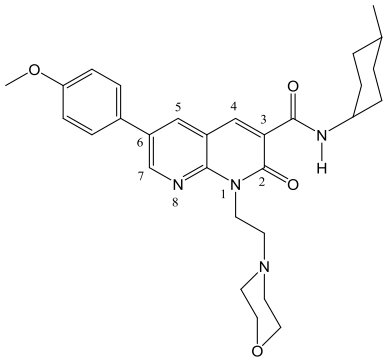

26

Figure 6. 1,8-Naphthyridine Agonists and Antagonists

Project 2: The Aminoalkylindoles

The aminoalkylindole (AAI) pravadoline was developed in hopes of producing a non-acidic non-steroidal anti-inflammatory drug (NSAID) that would lack negative gastrointestinal side effects [23]. In this process, it was discovered that pravadoline inhibits prostaglandin synthesis, a characteristic of other NSAIDs; and showed antinociception capabilities in rodent assays. Other AAI analogs showed antinociception activity in rodent assays, but did not inhibit prostaglandin synthesis, meaning they are producing antinociceptive effects by a different mechanism than NSAIDs. These AAI compounds and pravadoline were tested for their ability to inhibit electrically stimulated contractions of mouse vas deferens (MVD) preparations, an assay at which both opiod and cannabinoid receptors are active. It was found that pravadoline and these select analogs did have activity in the MVD assays, but this activity was not inhibited by the opioid antagonist naloxone. So, some AAIs have antinociceptive activity, but do not

inhibit prostaglandin synthesis or bind to the opioid receptors [24]. Shortly afterwards, the AAIs were found to inhibit adenylyl cyclase by acting through a G_i protein [25]. Along with many other GPCRs, the cannabinoid receptors produce effects mediated by Gi coupling [26]. AAI activity was tested at a number of different receptors thought to be capable of producing antinociceptive effects. It was found that AAIs do not act through opioid, purinergic, adrenergic, γ-aminobutyric acid, 5-HT, neurokinin, bradykinin, and prostanoid receptors [27]. This same study showed that AAIs have a similar profile as levonantradol, a cannabinoid agonist. It was soon found that AAIs act as agonists at the cannabinoid receptor [28, 29]. These experiments showed that the AAI, WIN55212-2 had the highest affinity for the cannabinoid receptor of all the AAIs. Once the CB2 receptor was discovered and cloned, it was shown that WIN55212-2 had a slightly higher affinity for CB2 than for CB1 [30].

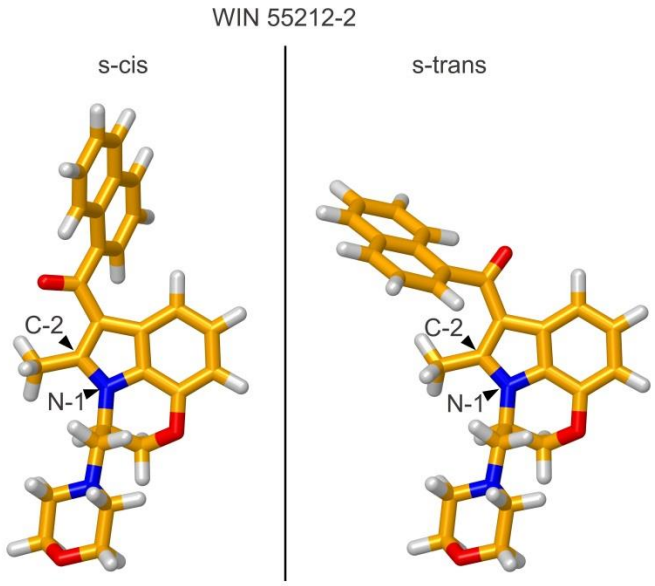

Figure 7. WIN 55212-2 s-cis and s-trans conformations

Bell et al. reported in 1991 the two important conformations, s-cis and s-trans, which AAI compounds can have due to positioning of the 3-naphthyl group [24]. Figure 7 shows the s-cis and s-trans conformation for WIN 55212-2. The s-cis conformation has the naphthyl group over the 6 membered ring of the indole and s-trans conformation has the naphthyl over the C-2 position of the indole. Conformational analysis of the AAI showed that when there is a methyl at the C-2 position the s-cis conformation is the lower energy conformation, but when there is a hydrogen at C-2 the s-trans conformation is lower in energy. Reggio et al. performed conformational analyses and receptor model docking studies of WIN 55212-2. These studies suggested that although the s-cis conformation of WIN 55212-2 is lower in energy, it is the s-trans conformation that is the preferred conformation for CB1 and CB2 [31]. These docking studies also suggested that the carbonyl group in WIN 55212-2 was not a receptor interaction site. To this this, they synthesized rigid (E)- and (Z)-naphthylidene indene analogs. The (E) isomer mimics the s-trans conformation and the (Z) isomer mimics the s-cis conformation. In these analogs, the carbonyl group has been removed and a double bond (cis or trans) has been incorporated in this region of the molecule. Binding studies of these analogs showed that the E-indenes had higher affinity for the CB1 and CB2. The (E) C2- H indene had a CB1 Ki of 2.72 nM and a CB2 Ki of 2.72 nM. The (E) C2-Me indene had a CB1 Ki of 2.89 nM and a CB2 Ki of 2.05 nM. The (Z) C-2 H indene had a CB1 Ki of 148 nM and a CB2 Ki of 132 nM. The (Z) C-2 Me indene had a CB1 Ki of 1945 nM and a CB2 Ki of 658 nM. These results also suggest that the carbonyl oxygen of the AAI's is not necessary for binding to the CB receptors. Reggio et al. reported that the most significant

interactions of WIN 55212-2 at the CB receptors were aromatic stacking interations in the TMH4-5-6 aromatic cluster region in CB1/CB2 [31]. Figure 8 shows the Z and E C-2 H indenes. Figure 9 shows the Z and E C-2 Me indenes.

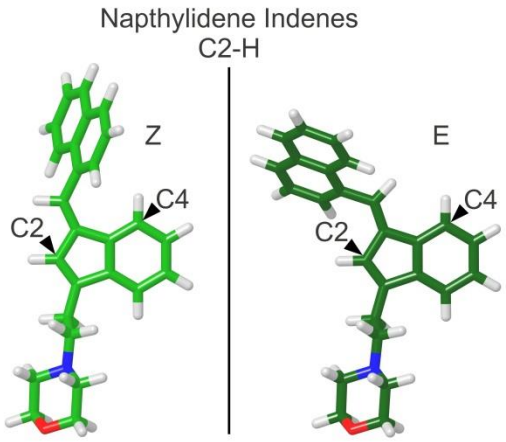

Figure 8. C-2 H (Z) and (E) indenes.

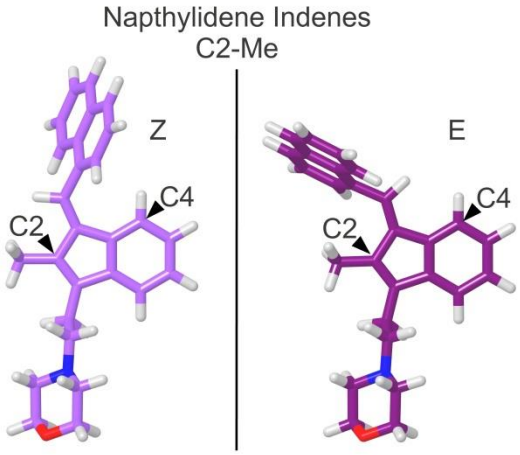

Figure 9. C-2 Me (Z) and (E) indenes

Data for WIN55212-2 binding to a non-cannabinoid receptor has been available for over 10 years. A study done in 1997 compared WIN 55212-2 binding in rat cerebellar membrane to neuroblastoma×glioma hybrid NG108-15 membranes (these latter membranes contain a low concentration of CB receptors). This study showed that known cannabinoid ligands did not displace [^{3}H]WIN55212-2 in NG108-15 membranes. Specifically, 5 μM of CP 55940 and AEA displaced only 15 % of [H^3]WIN55212-2 in these preparations. In rat cerebellar membranes (which contain a higher concentration of CB1 receptors), CP 55940 and AEA had IC_{50} values of 1 nM and 300 nM, respectively [32]. This same study showed that at 1 μM of Δ^9-THC or levonantradol did not displace [^{3}H]WIN55212-2 in NG108-15 membranes. While, other AAI analogs did displace [^{3}H]WIN55212-2 in NG108-15 membranes. This study concluded that there is a non-cannabinoid receptor found in NG108-15 cell membranes that selectively binds AAI ligands.

Ultimately, WIN 55212-2 has been shown to bind also to non-CB receptor [19, 33]. In collaboration with Dr. Nephi Stella's lab (from the University of Washington), the binding of WIN 55212-2 and other AAIs binding to a non-CB receptor is explored in this thesis.

Aminoalkylindole Binding Data

A collaborator of the Reggio Lab, Dr. Nephi Stella and his group have produced data showing WIN 55212-2 and other AAIs have activity *in vitro* at non-CB receptors in human embryonic kidney cells (HEK293) and astrocytoma cells (T98G) (unpublished).

The first interesting piece of evidence is mRNA data showing that neither cannabinoid receptors are present in HEK293 cells. This agrees with another experiment using microarray techniques to measure mRNA levels for hundreds of GPCRs in HEK293 cells [34]. These studies show that both cannabinoid receptors are not significantly expressed endogenously in HEK293 cells. WIN55212-2 displaces [^{3}H]WIN55212-2 in radioligand binding assays in untransfected HEK293 cells, while other known cannabinoid ligands do not. The ligands tested were Δ^9-THC, cannabidiol, cannabichromin, cannabinol, cannabigerol, HU-210, O-2050, SLV319, SR144528, AM630. Another piece of evidence showing non-CB receptors in HEK293 cells is that CP55940, a high affinity ligand for both CB receptors, SR141716, a high affinity CB1 ligand, and SR144528, a high affinity CB2 ligand, all do not displace [^{3}H]CP55940 in untransfected HEK293 cells. Experiments were done to rule out other receptor targets genetically related to the CB receptors that have been known to bind cannabinoid ligands. These experiments ruled out GPRs 3,6,12, 18, 35, 40, 55, and 120. Other receptors that were ruled out were 5-HT, β-adrenergic, TRPV1, LPA, P2Y, and S1P. All of this data points to the notion that there are AAI sensitive receptors that are non-CB receptors in HEK293 cells. To determine if these receptors are GPCR's a [^{35}S]GTPγS binding assay was performed. [^{35}S]GTPγS is a non-hydrolyzable form of GTP, so when it binds to the Gα subunit it will not be hydrolyzed back to GDP by GTPase. An increase in [^{35}S]GTPγS binding means the receptors are undergoing the GDP to GTP exchange. So these receptors are GPCRs. It was shown that AAI compounds increase [^{35}S]GTPγS binding in non-transfected HEK293 cells, suggesting that the non-CB site WIN 55212-2 binding site is a GPCR.

Pertussis toxin is used to determine if a GPCR couples to $G_{i/o}$ proteins. Pertussis toxin is known to inhibit any $G_{i/o}$ proteins in the cell from binding to GPCRs via ADP-ribosylation of the α subunit [35]. If a GPCR acts via $G_{i/o}$ proteins, adding pertussis toxin will eliminate any signaling. In this case pertussis toxin was shown to eliminate [^{35}S]GTPγS binding, thus these AAI receptors are coupling to $G_{i/o}$ proteins. The CB antagonists SR141716 and SR144528 do not block GTPγS binding, further suggestin that these AAI receptors are not CB receptors. In T98G cells it was shown that CP55940, SR141716A, and SR144528 do not displace [^{3}H]WIN55212-2, but other AAI compounds do. It was also seen in T98G cells that AAI compounds increase [^{35}S]GTPγS binding and this binding is sensitive to pertussis toxin. **Overall, this data suggests that AAI compounds are binding to non-CB receptors that are GPCRs which act via $G_{i/o}$ proteins in HEK293 and T98G cells.** Dr. Stella's group developed AAI analogs and tested their binding in HEK293 cells and T98G cells. We used this data to build a pharmacophore model for this non-CB AAI receptor. Figure 10 shows the structures of some of the AAI compounds used in this thesis. Table 4 in Appendix 2 shows the rest of the compounds used to develop a pharmacophore model and their binding affinities.

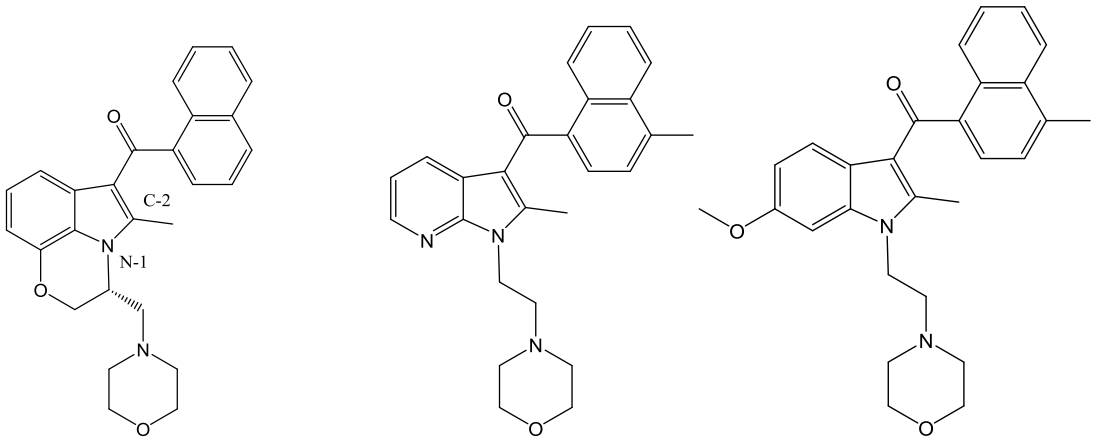

WIN 55212-2 CBX-003 CBX-006

Figure 10. Structures of Some AAI Compounds

Dr. Stella's group also used the previously mentioned, rigid (E)- and (Z)- indene analogs (Pages 13 and 14) to probe which conformation was active at the AAI binding sites. The C2 methyl Z-Indene had a Ki of 466 nM, while the C2 methyl E-Indene had undetectable binding. The C2 hydrogen Z-Indene had a Ki of 437 nM, while the C2 hydrogen E-Indene had a Ki of 3.4 μM. This data suggests that the (Z) isomer is preferred, thus the s-cis conformation is favored over the s-trans.

Dr. Stella's lab tested AAI analogs to develop SAR data for binding to these novel receptors. The SAR data showed that to bind to the AAI site the s-cis conformation is preferred, the accessibility of the carbonyl oxygen is important, the indole ring is important, and the naphthyl group is important. From the SAR data Dr. Stella's lab synthesized more AAI analogs to test, using these analogs and their binding data a pharmacophore model will be developed. To characterize the binding site and how

the ligands bind, one goal of this thesis is to develop a pharmacophore model for the non-CB AAI receptor. The goal of this study is to develop a pharmacophore that can be used to generate more selective ligands for these sites and to further characterize the pharmacology of these receptors.

CHAPTER II

GOALS AND METHODS

Project Goals

There are two goals for this project. 1) Create a binding model that explains how the 1,8-naphthyrdine analogs developed by Dr. Manera bind to CB2. 2) Create a pharmacophore model hypothesis for aminoalkylindoles binding to a unique GPCR found in HEK 293 and T98G cells.

Project 1: 1,8-Naphthyridine Binding Model Development

To help explain how these compounds are interacting with the receptor a docking study was performed using the automatic docking program Glide v5.8 (Schrodinger Inc., Portland, OR) [36, 37]. Before allowing Glide to dock the ligands, a thorough conformational search of each ligand was performed using Spartan '08 (Wavefunction Inc., Irvine, CA). All of the rotatable bonds in each ligand were identified and rotated 3-8 fold. A semi-empirical AM1 geometry optimization was performed on all of the conformers generated from these rotations. After this initial geometry optimization all duplicates were deleted. A more rigorous, *ab initio* geometry optimization was performed using Hartree-Fock level of theory at the 6-31G* level for **A1**, **A2**, **5**, **17**, and

26; and 6-311G* basis set was used for compounds **20** and **21** to account for the bromine atom. This identified the global minimum conformer for each ligand, which was used as the starting structure in Glide v5.8 for the docking process.

To generate the docked complexes, the ligands were first docked using interactive computer graphics into the CB2 model. The CB2 model was pulled from molecular dynamics simulation of CB2 with its endogenous ligand 2-AG. The agonists were docked into the active state model, which had the toggle switch residues in the appropriate conformations and the salt bridge between the ionic lock residues were broken. The antagonists were docked into the inactive state model with an intact salt bridge and appropriate conformations for toggle switch residues. The transmembrane helices were pulled apart and the ligands were placed into the active site. The ligand-receptor complexes were minimized using the OPLS2005 all atom force field in Macromodel 9.9 (Schrodinger Inc.). Glide v5.8 was used to explore the other possible ligand conformations and receptor interactions using flexible docking. Flexible docking allows Glide to translate the ligand in the receptor and rotate ligand dihedrals to find the best ligand conformation. Certain residues were constrained to interact with the ligands. Based on mutation data [38], S7.39 was required to be in a hydrogen bonding interaction with the ligand and hydrophobic residues in contact with the ligand were noted as important interactions for the flexible docking.

Project 2: Pharmacophore Model Development for the AAI Receptor

A pharmacophore model is a set of chemical features and their spatial arrangements that describe how a set of ligands bind to a biological target. To make a pharmacophore model a conformational search on active and inactive ligands must be performed to understand the conformational space the ligands are occupying. A conformational search of subject AAI compounds was performed in Spartan '08 (Wavefunction, Inc.). All compounds were built in Spartan '08 and all the rotatable bonds were identified. The bonds connecting both aromatic groups to the carbonyl carbon were set to an 8 fold rotation. The rotatable bond connected to the N-1 position was set to a 2 fold rotation. The next bond in the tail was set to a 3 fold rotation. A geometry optimization of all of the conformers that were generated was performed in Spartan '08 using the semi-empirical AM1 level of theory. After this, the conformers were examined to identify all unique conformations. These unique conformers were used to further refine the conformational search via geometry optimizations at the Hartree-Fock level 6-31G* level. After this calculation was performed the duplicate conformers were deleted to leave only the unique conformations of the molecule. These unique conformers were used to develop the pharmacophore model for aminoalkylindoles binding to the AAI sites using the program PHASE v3.4 (Schrodinger Inc., Portland, OR.) [39].

Before PHASE was used, as much information was gathered on what features of compounds appear to produce binding vs. what features appear to interfere with binding.

Based on the Indene binding data (see Page 17) it is clear that the bioactive conformation is the s-cis conformation. The Z indenes bind with a higher affinity than the E-indenes, thus the s-cis conformation is preferred. Also, based on the binding data for WIN 55212-3, the S enantiomer, it is known that the N-1 tail prefers to be on one side of the indole ring. This data was taken into consideration when developing the pharmacophore model in PHASE. Only the s-cis conformers were put into PHASE, and any pharmacophore hypothesis generated with the N-1 tail on the wrong side of indole will not be considered.

In PHASE, compounds with a Ki value under 5 nM were identified as active compounds. This gave five compounds, WIN 55212-2, TK 18, CBX 003, CBX 004, and CBX 009 (see Appendix 2 Table 4) as active. The pharmacophore model was generated from the s-cis conformation of these active compounds. CBX 008 was assigned as inactive because of its high Ki value of 972 nM. Chemical features were assigned to the ligands based on the algorithm PHASE uses. The features are aromatic (R), hydrogen bond acceptor (A), hydrogen bond donor (D), hydrophobic (H), positive (P), and negative (N). These features can be removed or features can be added. PHASE assigned the nitrogen on the morpholino ring a positive (P) feature, meaning it will be protonated at physiological pH. However, the pKa of these compounds is in the range of 4.5-6.0 [28], so these compounds will not be protonated at physiological pH. The positive feature on the morpholino nitrogen was therefore removed and was not used in generating the pharmacophore model. All other features were left how PHASE assigned them. All of the compounds had four aromatic features due to the two rings of the indole ring and the two rings of the naphthalene. All compounds had a hydrogen bond acceptor feature due

to the carbonyl oxygen attached at C-3 of the indole ring. All compounds had a hydrophobic feature at the N-1 tail, but these hydrophobic features were not in the same exact region of space for all compounds. WIN 55212-2 had a hydrophobic feature shifted from the rest of the active compound's N-1 hydrophobic feature. This made it impossible for PHASE to incorporate a hydrophobic feature in the final pharmacophore model. The maximum number of sites and the minimum number of sites was set to 6, so the model will have 6 features in it. The common pharmacophore hypotheses were assigned to match all five active compounds. To generate the common pharmacophore hypotheses PHASE uses a tree based partitioning technique using the intersite distances of pharmacophores. The options of finding a common pharmacophore were left at their default values which are a minimum intersite distance of 2.0 Å, a maximum tree depth of 5, an initial box size of 32.0 Å, and a final box size of 1.0 Å. Once the common pharmacophore hypotheses were determined, a survival score was calculated for each. The survival score was used to rank the pharmacophore hypotheses. The survival score involves the Reference_Score, a Volume_Score, a conformational energy factor, and how well the hypothesis matches a specified number of active compounds. This survival score was further refined by assessing how well the hypothesis aligns to inactive compounds. If an inactive compound aligns well, then the survival score is penalized. A higher survival score corresponds to a better pharmacophore model and helps decide which hypothesis is the best model. The pharmacophore model that was used had the highest survival score.

CHAPTER III

RESULTS

Project 1: Conformational Analysis of 1,8-Naphthyridine Compounds

The conformational search on the 1,8-naphthyridine compounds (see Appendix 2 Table 3 for structures) revealed several key common features. The 4-methyl cyclohexyl group attached to the amide gave rise to four positional isomers (see Figure 11). There are two cis isomers and two trans isomers. One cis isomer has the amide group positioned axial and the 4-methyl positioned equatorial. The other cis isomer has the amide equatorial and the 4-methyl axial. The two trans isomers have both groups positioned either axial or equatorial. The lowest energy isomer is the trans isomer with both groups positioned equatorial. The other trans isomer is 3.4 kcal/mol higher in energy. The cis with the amide equatorial is 2.2 kcal/mol higher and the cis with the amide axial is only 1.1 kcal/mol higher in energy. Manera et al. reported in 2009 that the cis isomer has a 0.7 nM affinity for CB2, while the trans isomer has a 9.0 nM affinity [40]. The lowest energy conformers with the 4-methyl cyclohexyl group positioned in a cis conformation with the amide group axial were used in this docking study. Figure 11 shows the four positional isomers and their relative energies for compound **A**.

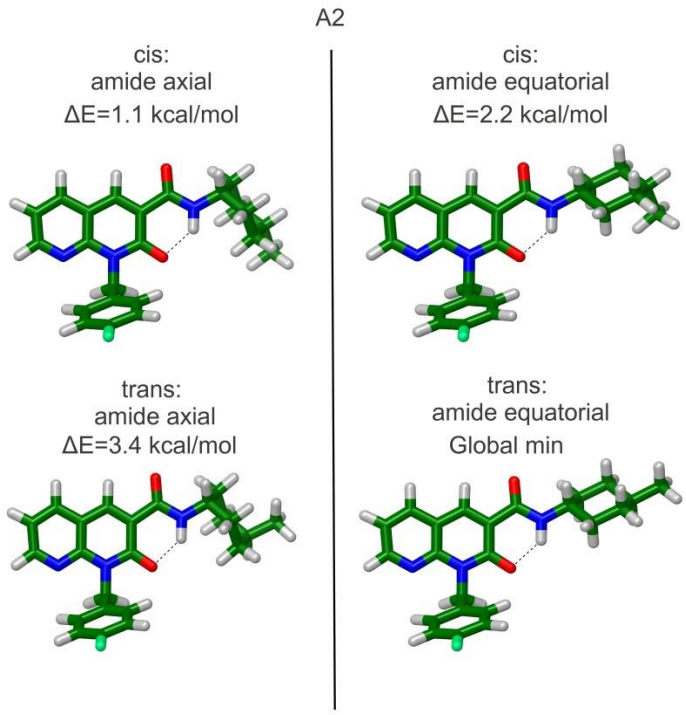

Figure 11. The Four Positional Isomers and Their Relative Energies for Compound **A2**

Another common feature for these ligands is that they all have an intramolecular hydrogen bond between the amide N-H and the carbonyl carbon on C-2 (see Appendix 2 Table 3 for drawing). For this hydrogen bond to be in place the amide group must be in plane with the naphthyridine ring. If the amide is rotated 30 degrees out of plane, there is a significant energy increase of 2.0 kcal/mol. To rotate the amide a full 90 degrees out of plane costs 8.14 kcal/mol. It is important to know the energy cost associated with this rotation because it is unlikely that a docked conformation can have the amide rotated out of plane with the naphthyridine ring. Any Glide result with the amide rotated out of plane can be discarded because of the high conformational cost associated with losing the

internal hydrogen bond. Figures 12 and 13 show the global minima conformers for the agonists and antagonists, respectively.

Compound **5** adopts a unique global minimum conformation due the 4-hydroxy butyl tail attached at N-1 (see Figure 12). The hydroxyl group is able to form an additional intramolecular hydrogen bond with the carbonyl oxygen at C-2. To lose this additional internal hydrogen bond costs 1.5 kcal/mol.

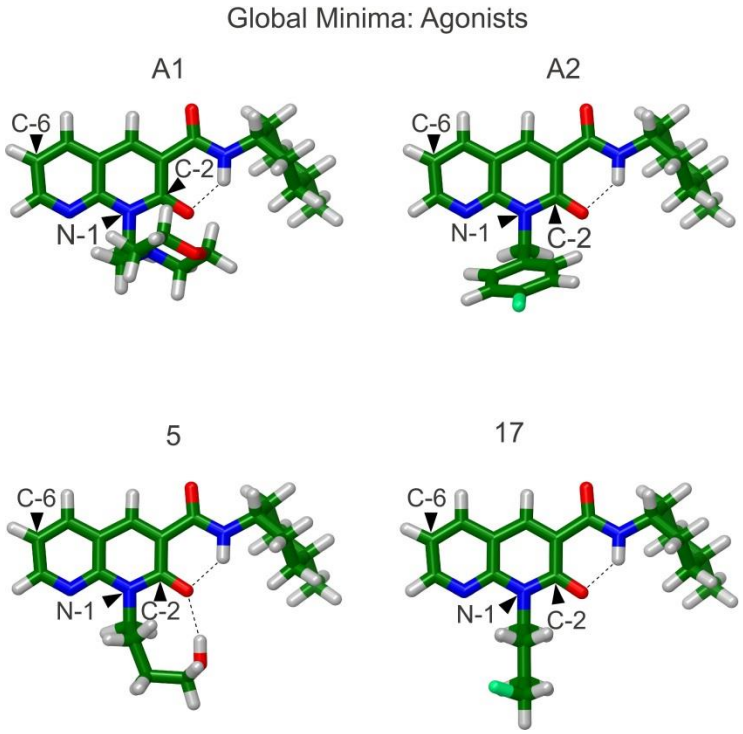

Figure 12. Structures of the Global Minima for 1,8-Naphthyridine Agonists. The dotted line represents intramolecular hydrogen bonding.

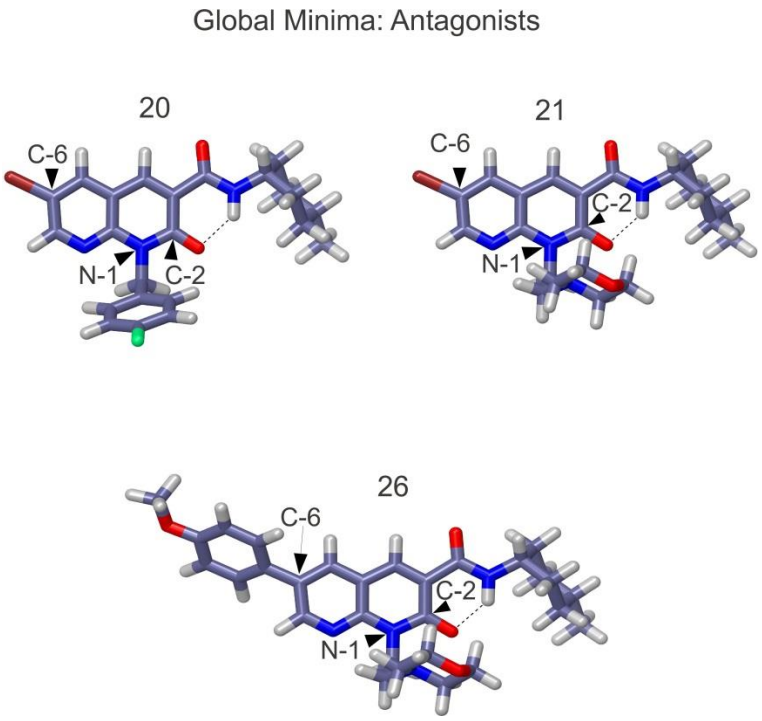

Figure 13. Structures of the Global Minima for 1,8-Naphthyridine Antagonists. Compound **20** and **21** have a Br at C-6 and Compound **26** has a p-methoxyphenyl at C-6. The dotted line represents intramolecular hydrogen bonding.

Docking Results of 1,8-Naphthyridine Compounds

The docking results for all of the compounds showed hydrogen bonds with both, K3.28 and S7.39. K3.28 forms a hydrogen bond with the carbonyl oxygen on C-2 and S7.39 forms a hydrogen bond with the carboxamide oxygen. F2.57 is forming an aromatic-aromatic interaction with the 1,8-naphthyridine ring for all compounds. Residue F2.61 has a hydrophobic interaction with the 4-methyl cyclohexyl group. Residues I3.29, V3.32, M6.55, and L6.59 form a hydrophobic pocket in which part of the ligand sits. For the antagonists, compounds **20**, **21**, and **26**, the C-6 substituent extends down into the receptor far enough to block the "toggle switch" residue W6.48 from

changing its χ1 torsion angle from g+ to trans. This prevents the receptor from undergoing the conformational change associated with receptor activation and G-protein coupling. The agonists, compounds **A1**, **A2**, **5**, and **17**, bind to the receptor but cannot block W6.48 because they have smaller substituents at C-6. As a result, W6.48 can change conformations along with F3.36 (see Introduction, Page 3) causing the ionic lock between TMH3 and TMH6 to break, and creating an intracellular opening for G-protein insertion. All compounds have aromatic-aromatic interactions and hydrophobic interactions with the same set of residues. Figure 14 shows compound **A1**, an agonist, docked in the receptor. The dotted lines represent hydrogen bonds. Figure 15 illustrates compound **26**, an antagonist, docked in the receptor model. Both agonists and antagonists interact with receptor in similar ways, the difference comes from the space occupied by the C-6 substituent on the antagonists. Figure 16 shows the agonist **A1** binding to CB2 and how the absence of a substituent on C-6 allows for W6.48 to change conformations and activate the receptor for G-protein insertion. Figure 17 shows the antagonist, **26** and how its large substituent on C-6 blocks the conformational change of W6.48.

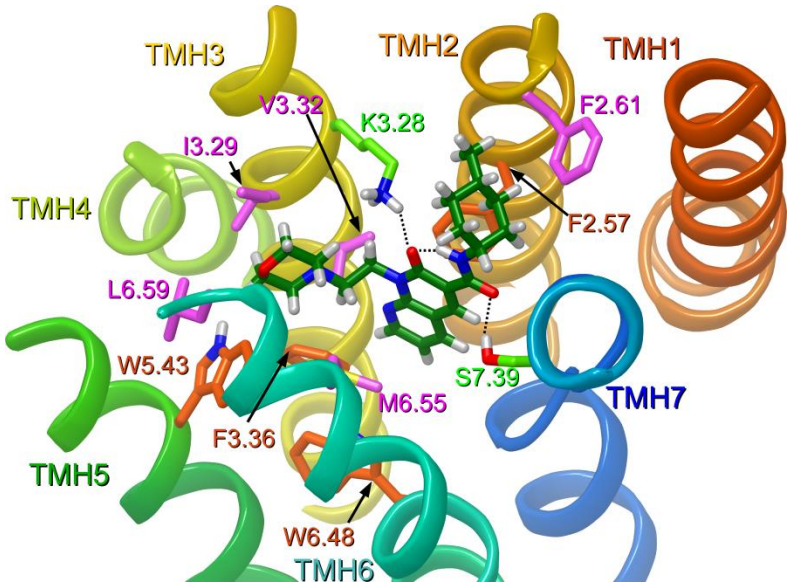

Figure 14. Binding Model of Agonist, Compound **A1** Docked into CB2. The view is from extracellular with loops removed for clarity. Pink residues are interacting via hydrophobic interactions, orange residues are interacting via aromatic-aromatic interactions, and green residues are hydrogen bonding.

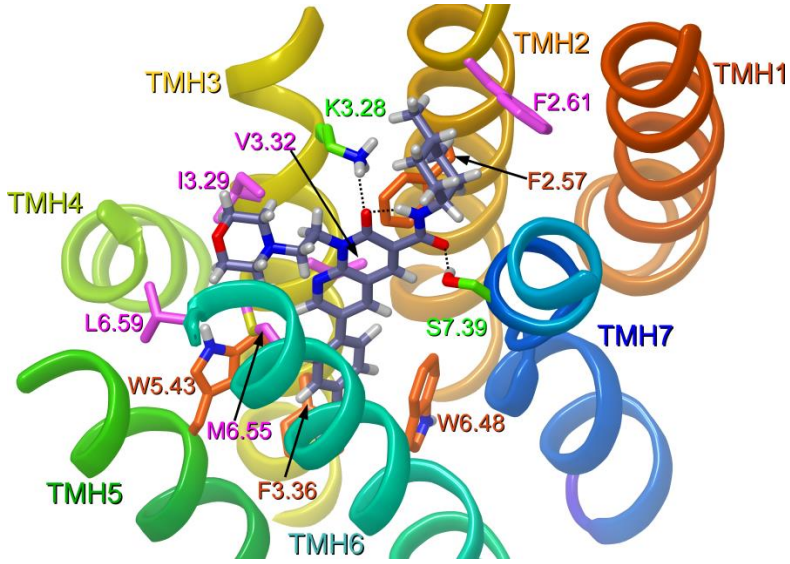

Figure 15. Binding Model of Antagonist, Compound **26** Docked into CB2. The view is from extracellular with loops removed for clarity. Pink residues are interacting via hydrophobic interactions, orange residues are interacting via aromatic-aromatic interactions, and green residues are hydrogen bonding.

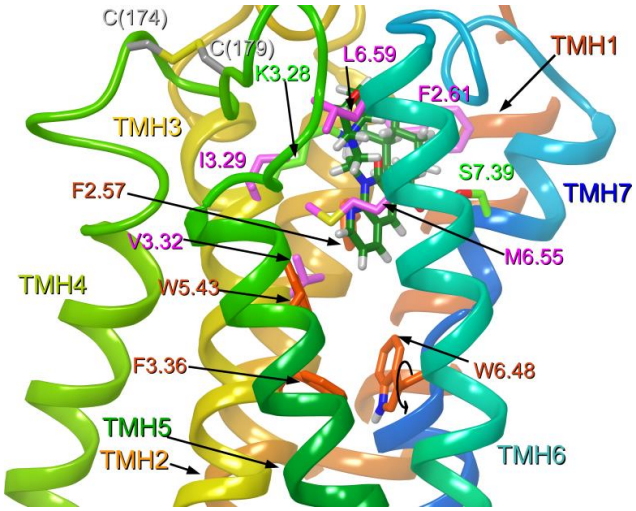

Figure 16. Transmembrane View of Binding Model of Agonist, Compound **A1** Docked into CB2. The view is from the transmembrane region. Pink residues are interacting via hydrophobic interactions, orange residues are interacting via aromatic-aromatic interactions, and green residues are hydrogen bonding. The black arrow on W6.48 shows the path its χ1 torsion angle takes during activation.

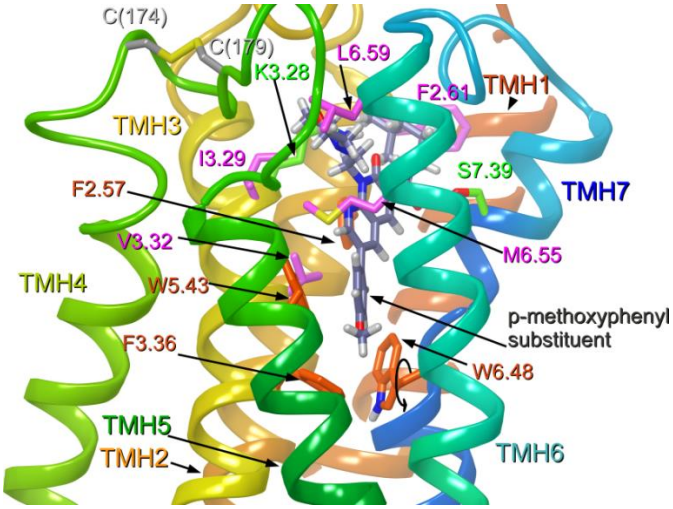

Figure 17. Transmembrane View of Binding Model of Antagonist, Compound **26** Docked into CB2. The view is from the transmembrane region. Pink residues are interacting via hydrophobic interactions, orange residues are interacting via aromatic-aromatic interactions, and green residues are hydrogen bonding. The black arrow on W6.48 shows the path it needs to take to activate. It is clear here that this change is blocked by the ligand.

Project 2: Aminoalkylindole Conformational Analysis

The unique conformers for the AAI compounds can be separated into two distinct classes. For each AAI compound there is an s-cis conformation and an s-trans conformation. The s-cis conformation places the naphthyridine ring over the indole ring and the carbonyl oxygen over the C-2 group, while the s-trans places the naphthyridine ring over the C-2 group and the carbonyl oxygen over the indole ring. When the C-2 group is a methyl the s-cis conformation is lower in energy than the s-trans. Figure 18 shows the s-cis and s-trans conformations for WIN55212-2 (which contains a C-2 methyl). It is also shows that the s-trans conformation for WIN55212-2 is 1.55 kcal/mol higher in energy. When the C-2 group is a hydrogen, the s-trans is lower in energy. Analyzing the conformational search of JWH 120, which has a hydrogen at C-2 shows that the s-trans conformation is lower in energy. Figure 19 shows the s-cis and s-trans conformations for JWH 120. The JWH 120 s-cis conformation is 1.81 kcal/mol higher in energy. JWH 120 is the only aminoalkylindole with a hydrogen at C-2 used in this study. As mentioned before, only the s-cis conformers were used to generate the pharmacophore model.

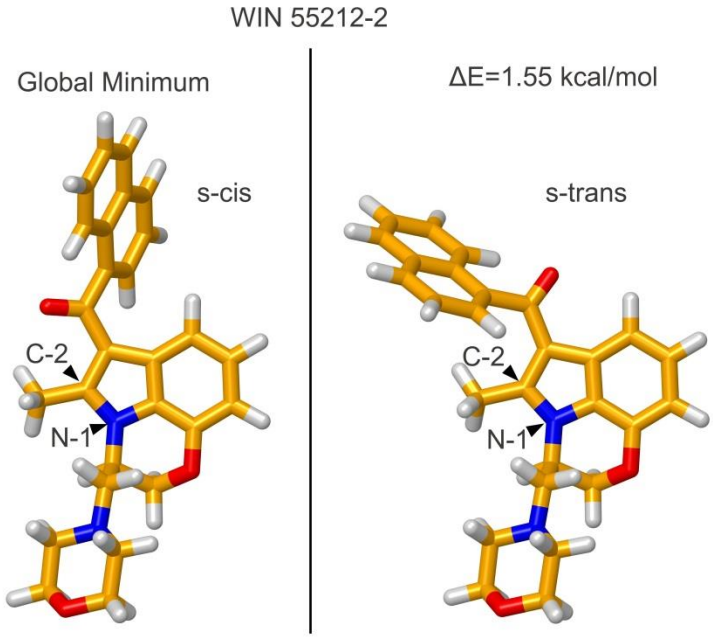

Figure 18. The s-cis and s-trans Conformations of WIN 55212-2. The s-trans conformation is 1.55 kcal/mol higher in energy.

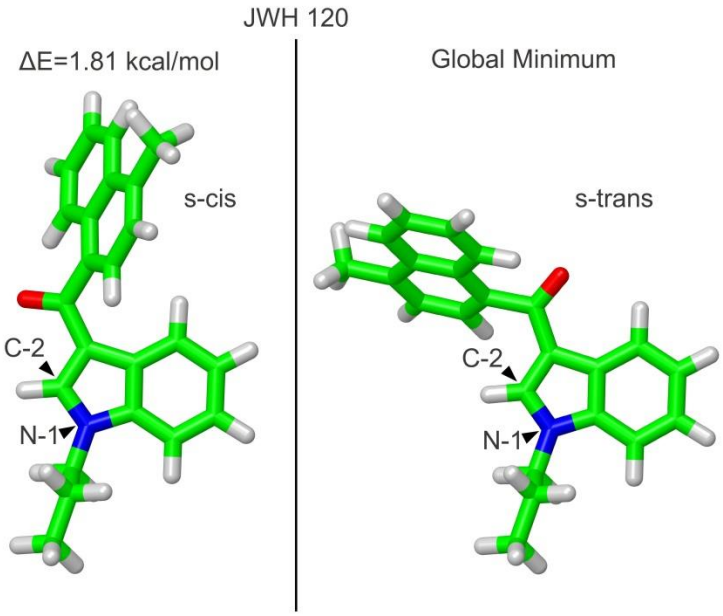

Figure 19. The s-cis and s-trans Conformations of JWH 120. The s-cis conformation is 1.81 kcal/mol higher in energy.

A high number of conformers arise due to the orientation of the naphthyl group and the dihedrals of the N-1 tail. The N-1 tail prefers to be in an extended conformation, making the second bond in the tail assume an anti conformation. There are four orientations the naphthyl group prefers to be in when the overall conformation is s-cis. For WIN 55212-2 the naphthyl group prefers to have it's B ring (the ring not directly connected to the carbonyl carbon) and the carbonyl oxygen on the same side as the N-1 tail. To put both on the opposite side of the the N-1 tail costs 0.044 kcal/mol. The other naphthyl ring conformations, put the B ring and the carbonyl oxygen on opposite sides. For the B ring to be on the opposite side as the N-1 tail and the carbonyl oxygen to be on the same side as the N-1 tail costs 1.31 kcal/mol. The reverse, costs 1.36 kcal/mol. The global minimum conformer for WIN 55212-2 has the carbonyl oxygen 21.3 ° out of plane with the indole ring. These four conformations of the naphthyl group for WIN 55212-2 are shown in Figure 20. The other AAI compounds have the carbonyl oxygen slightly more out plane with the indole ring in their global mins (25° - 30°). All of the other actives compounds prefer to have the B ring of the naphthyl group and the carbonyl oxygen on the opposite side of the indole ring as the N-1 tail. To put both groups on the same side as the N-1 tail costs, 0.100 kcal/mol for TK-18, 0.094 kcal/mol for CBX 003, 0.095 kcal/mol for CBX 004, and 0.452 kcal/mol for CBX 009. Figure 21 shows the naphthyl group conformations for TK 18.

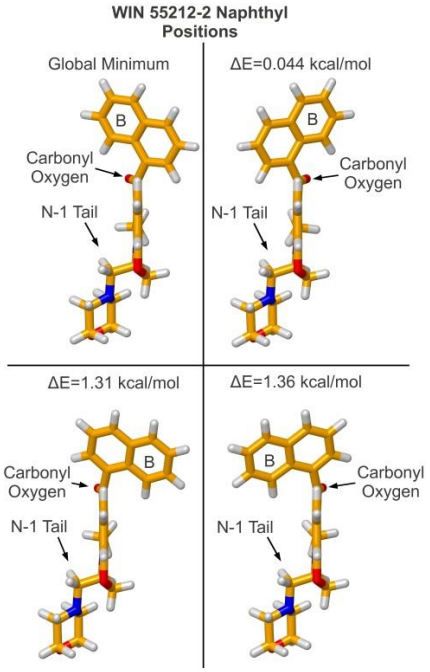

Figure 20. The Positions the Naphthyl Group Prefers to Assume in WIN 55212-2 and Energies.

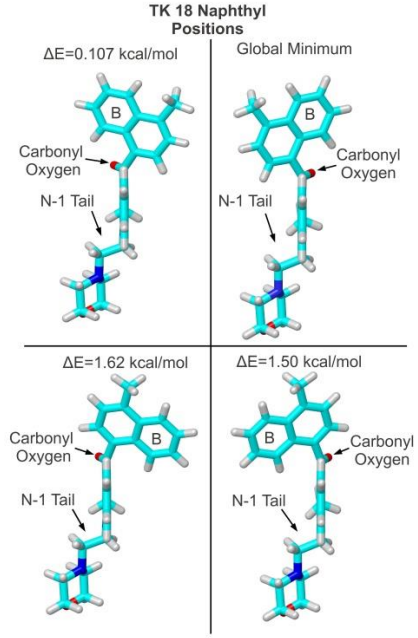

Figure 21. The Positions the Naphthyl Group Prefers to Assume in TK 18 and Energies.

The inactive compound, CBX 008 (structure and binding data in Appendix 2 Table 4), has its carbonyl oxygen 55.7° degrees out of plane with the indole ring. The C-2 trifluoromethyl group sterically hinders the oxygen from coming into plane. This causes the naphthyl group to occupy space that the s-cis conformers of the other AAI compounds do not occupy. Another inactive compoud, CBX 007, has a chlorine at C-4 of the indole. This Cl atom interferes with the naphthyl group when CBX 007 is in an s-cis conformation. This results in the carbonyl oxygen being 51° out of plane with the indole. Another inactive compound, CBX 001, has a methoxy group at C-5 of the indole ring. The methyl group prefers to point up towards C-4. The carbonyl oxygen is only 26° out of plane with the indole ring, similar to AAI compounds that bind. However, CBX 001 may have steric clashes with the receptor caused by the methoxy group at C-5.

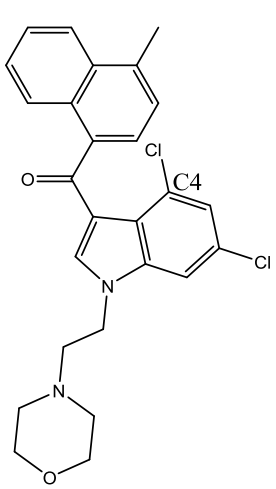

CBX 007

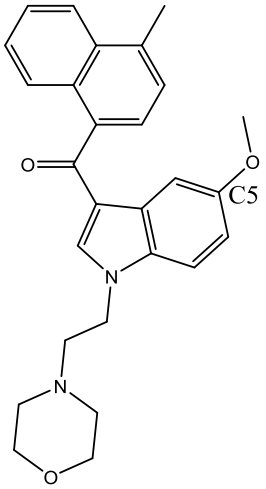

CBX 001

Figure 22. Structures of Inactive AAIs: CBX 007 and CBX 001

Amioalkylindole Pharmacophore Model

The final pharmacophore model (see Figure 23) has six features; four aromatic features, one hydrophobic feature, and one hydrogen bond acceptor feature. Two of the aromatic features correspond to the indole rings (R7 and R8) and the other two correspond to the naphthyridine ring (R9 and R10). The hydrophobic feature (H6) corresponds to the C-2 methyl group that is found on all of the actives and promotes the s-cis conformation. The hydrogen bond acceptor feature (A3) corresponds to the carbonyl oxygen. Figure 23 shows the pharmacophore model from the side and from behind the indole ring. Table 1 in Appendix 1gives the distances between the features in the model. Table 2 in Appendix 1 gives the angles between the features in the model. Because PHASE places the N-1 tail hydrophobic feature in slightly different region of space for WIN 55212-2 compared to the other actives, no hydrophobic feature was able to be placed at the N-1 tail. No analog has been tested to find the importance of a hydrophobic feature at the N-1 tail. The pharmacophore model places the B ring of the naphthyl group and the carbonyl oxygen on the same side of the indole ring as the N-1 tail. This orientation matches WIN 55212-2's global minimum conformation. This agrees with the binding data because WIN 55212-2 has the highest affinity for the receptor (Ki = 27 pM). Figure 24 shows WIN 55212-2 aligned to the pharmacophore model. All the features of the model align well with WIN 55212-2's global minimum conformation. Figure 25 shows TK 18, another active compound, aligned to the model. The conformation of TK 18 that aligns the best is 0.108 kcal/mol higher in energy than the global minimum. When aligning the model to the inactive compound it is expected to

not align well. Figure 26 shows CBX 008 aligned to the model and how the naphthyl rings do not align well to those two aromatic features. Also, the carbonyl oxygen is not aligned well with the hydrogen bond acceptor feature.

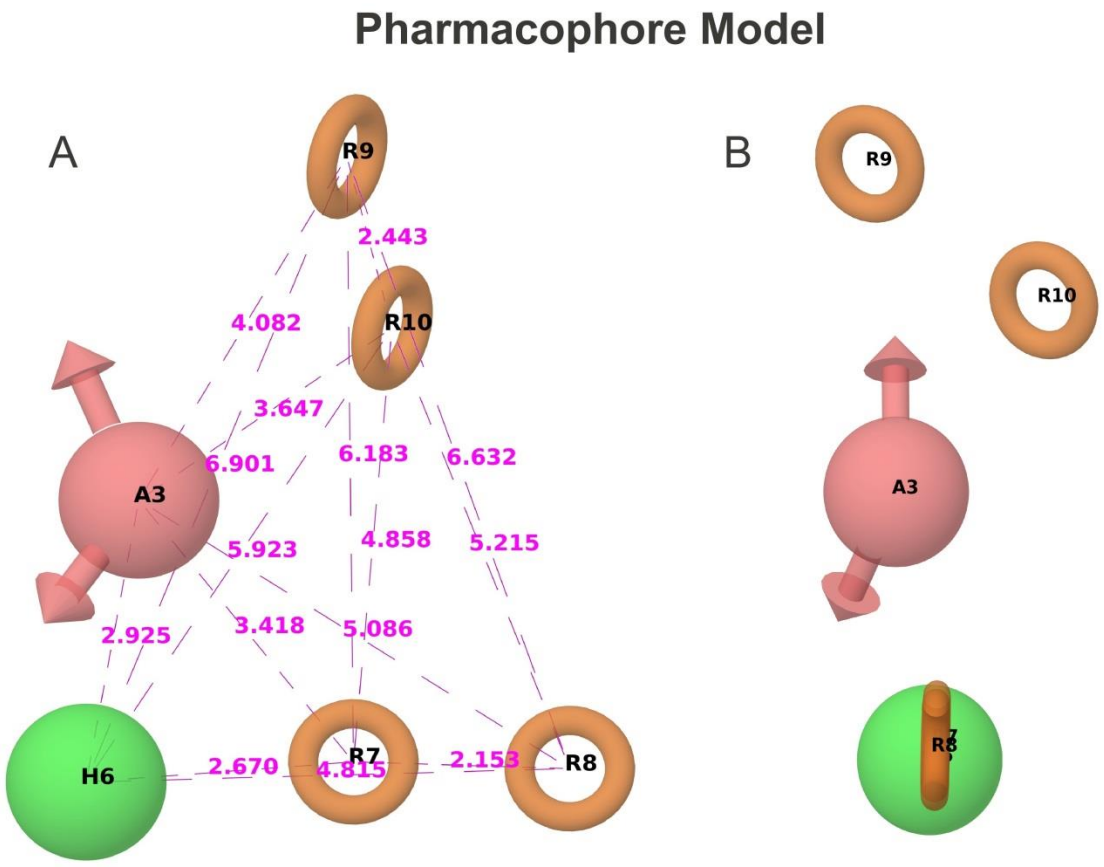

Figure 23. Pharmacphore Model. A) From the side view with distances B) Rotated 90° about the z-axis from image A to look behind the indole ring.

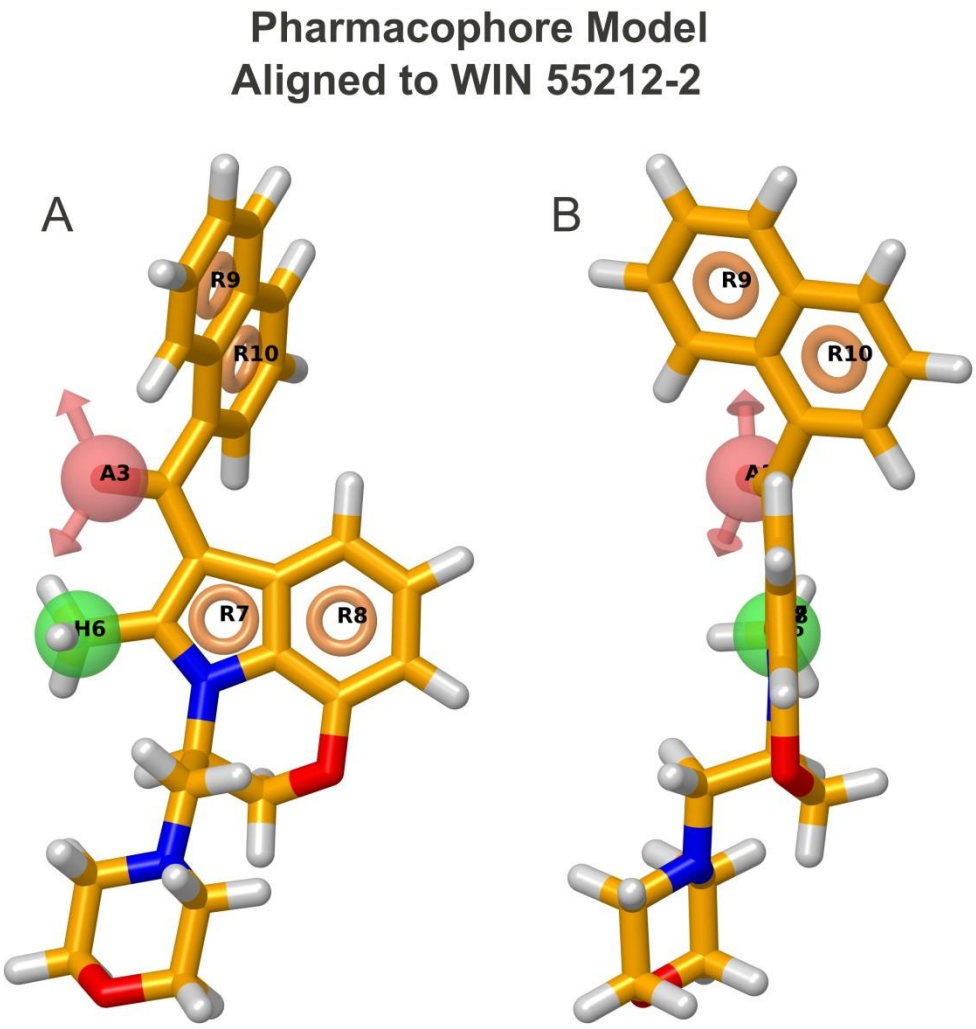

Figure 24. Pharmacophore Model Aligned to WIN 55212-2. A) Side view B) Rotated 90° about the z-axis from image A to look behind the indole ring.

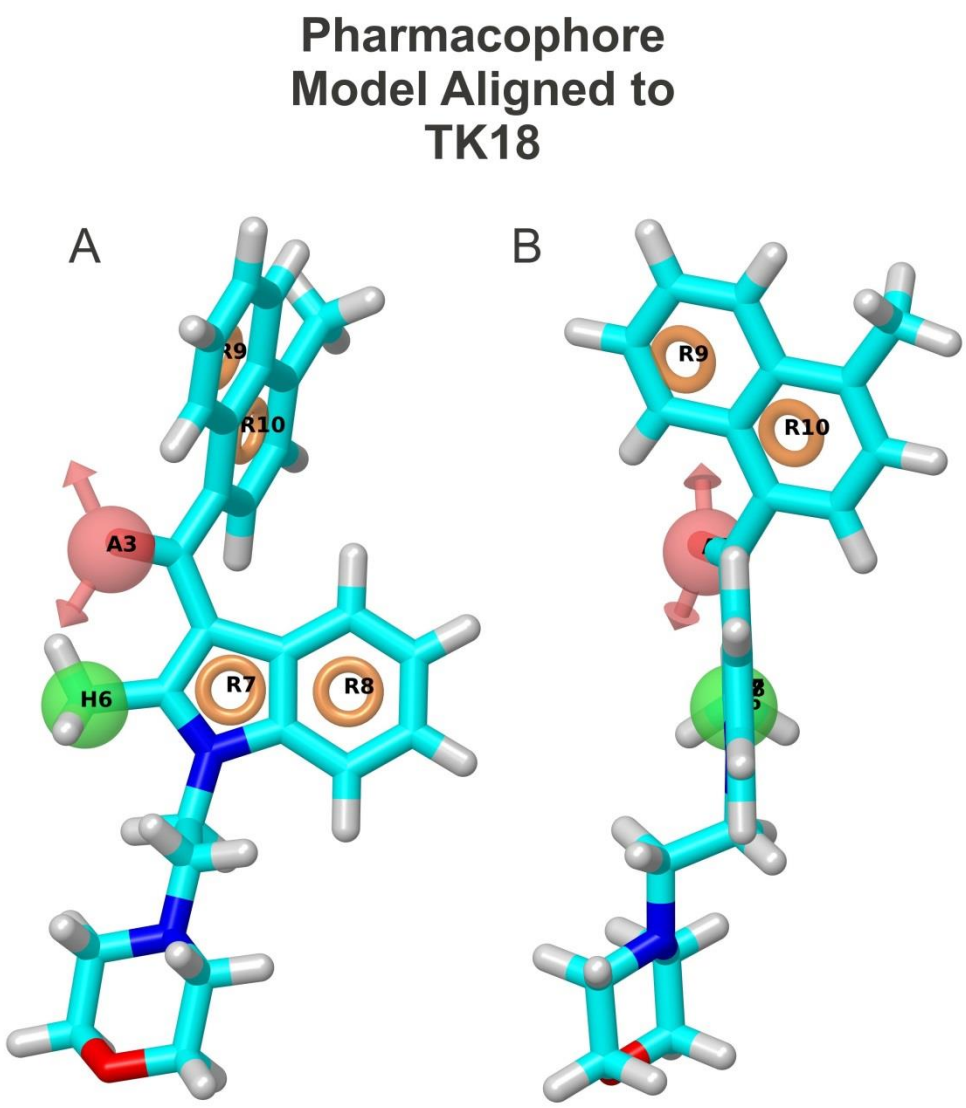

Figure 25. Pharmacophore Model Aligned to TK 18. A) Side view B) Rotated 90° about the z-axis from image A to look behind the indole ring.

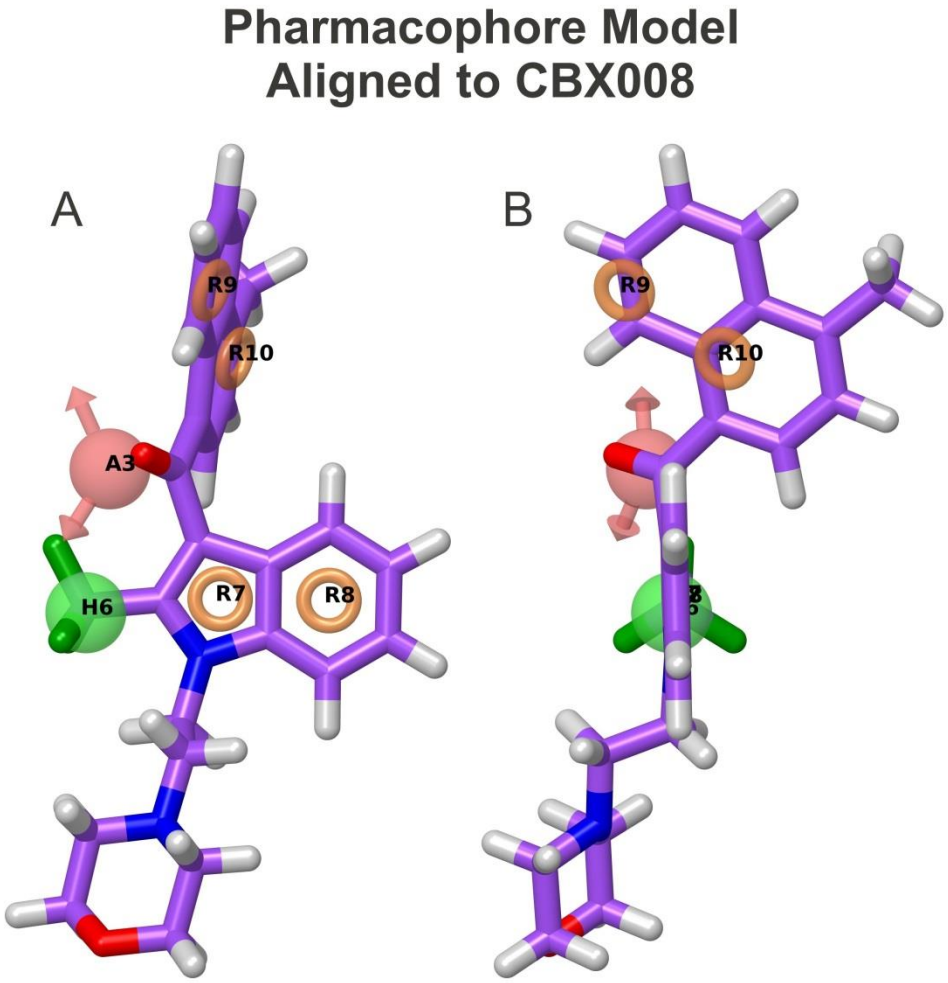

Figure 26. Pharmacophore Model Aligned to CBX 008. A) Side view B) Rotated 90° about the z-axis from image A to look behind the indole ring.

The poor aligment for CBX 008 is due to the trifluoromethyl group that causes steric clashes with the carbonyl oxygen and pushes the oxygen 55.7° out of plane. Figure 27 shows how far out of plane the carbonyl oxygen is in CBX 008 compared to WIN 55212-2.

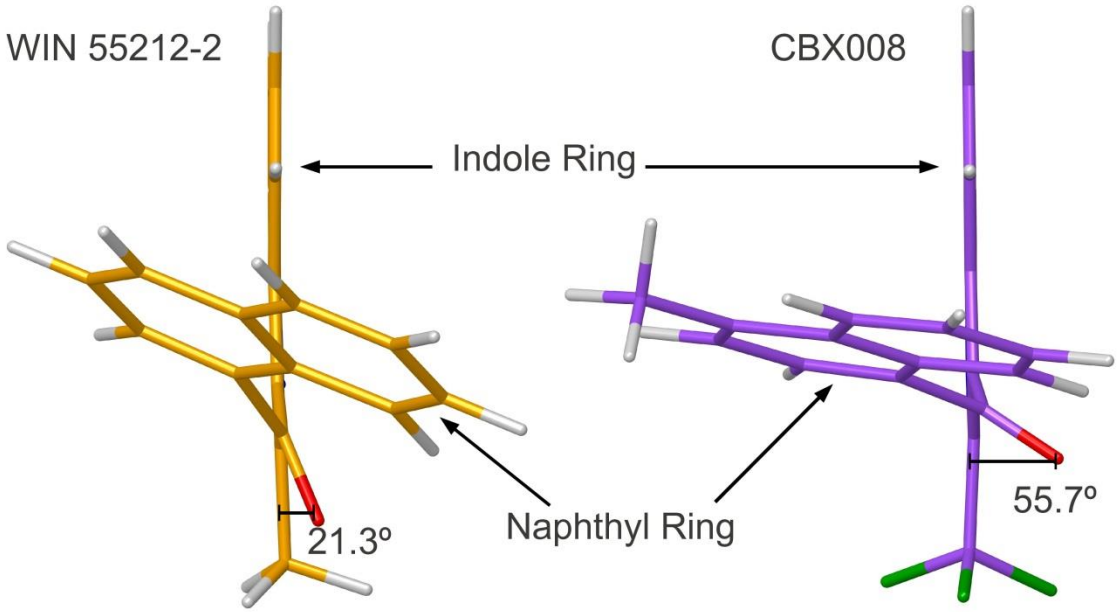

Figure 27. WIN 55212-2 vs. CBX 008: Carbonyl Oxygen Out of Plane.

Recommendations for Additional Analogs to be Tested

Having developed this first pharmacophore model for the AAI receptor, there are some analogs (not synthesized yet) that would help with a second generation model. When designing these analogs to test, it is important to not change too many groups at once. Some AAI analogs that have already been made and tested, changed two groups at once and therefore it is not possible to attribute loss of binding to a single reason.. WIN 55212-2 has the highest affinity for the receptor with a Ki of 27 pM. What makes WIN 55212-2 stand out as the best ligand should be further explored. Some additional analogs could be tested to determine this. The feature that WIN 55212-5 has that the other compounds do not is the heterocyclic ring fused to the indole ring. The ether group in that ring may be hydrogen bonding with the receptor, thus increasing the affinity. Table

1 shows two analogs that could be made and tested to determine the importance of that ether oxygen. Analog 1 has a ketone group at the C-7 position of the indole ring, putting a hydrogen bond acceptor group in a similar region of space as WIN 55212-2 does, but removing the fused ring. Analog 2 removes the ether oxygen from WIN 55212-2 and replaces it with a methylene group. How these substituents affect the conformation of the N-1 tail would need to be explored as well. Table 2 shows a set of analogs that could be made and compared to TK 18 (Ki 0.8 nM). The importance of a hydrophobic group at N-1 is not clear because there was no analog tested that did not have a hydrophobic group at N-1. Existing analogs show that a methyl, ethyl, propyl, cyclopropyl, trifluoroethyl, and ethylmorpholino groups at N-1 all have affinity for the receptor. Analog 3 has just a hydrogen at N-1, this analog would test if a hydrophobic group is necessary for binding. Analog 4 removes the six member ring of the indole to leave a pyrrole ring. This would test the neccessity of the indole ring. The ethylmorpholino ring at N-1 could be interacting via hydrogen bonding with the receptor or it could be interacting via hydrophobics interactions. To probe the role of the ethylmorpholino ring in AAI binding, Analog 5 could be made with an N-1 ethyl cyclohexyl group. The AAI compound Pravadoline is inactive at this receptor. Is this due to the loss of the extra 6 member ring of the napthyl or because of the methoxy group at the C-4 position? To test this, Analog 6 could be made with a methoxy at C-4 of the naphthyl group. Analog 7 has an anthracene group attached to the carbonyl carbon instead of a naphthyl group. There is a methyl group at the C-6 position to mimic the methyl group at the C-4 position in TK 18.

Analog 7 would probe how large the binding site is and if increasing the aromatic groups increases affinity.

Table 1. Analogs to be Tested from Parent Compound WIN 55212-2

Parent Compound	Analog 1	Analog 2
WIN 55212-2 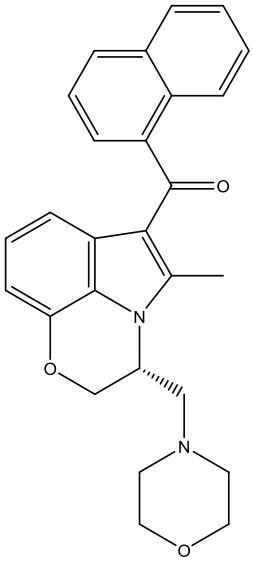	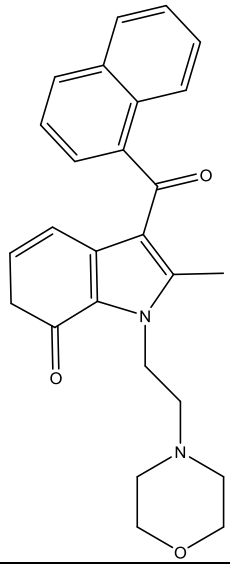	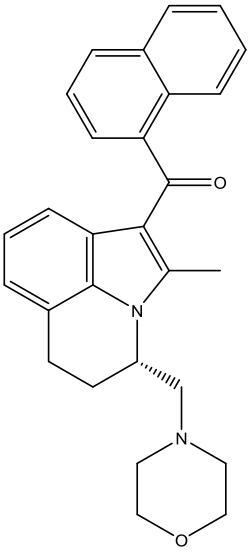

Table 2. Analogs to be Tested from Parent Compound TK 18 and Pravadoline

Parent Compound	Analog 3	Analog 4	Analog 5	Analog 6	Analog 7	Pravadoline
TK 18 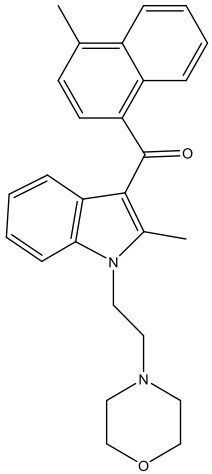	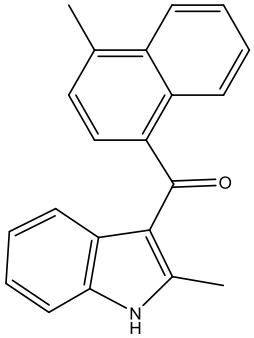	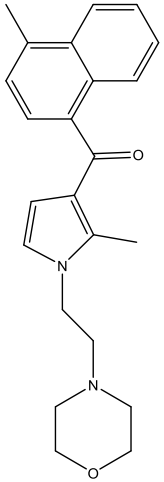	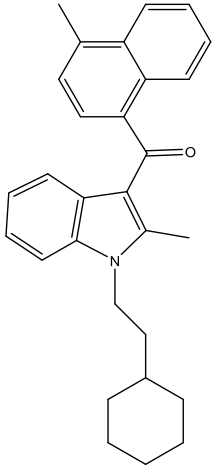	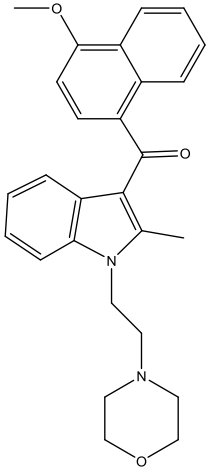	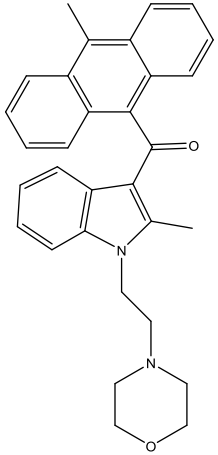	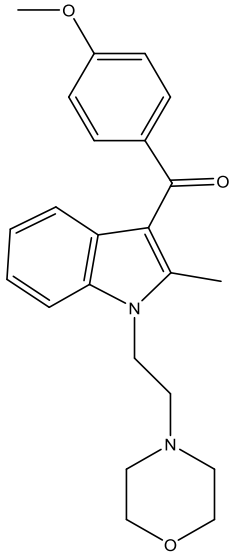

CHAPTER IV

CONCLUSION

Project 1: 1,8-Naphthyridine Binding Model

Compounds from the 1,8-naphthyridine scaffold were developed in hopes of generating CB2 selective ligands. Ligands were successfully developed that are selective for CB2, but some of these compounds act as agonists and some act as antagonists/inverse agonists. A binding model was developed to explain the different activities. The binding model shows that compounds with a substituent attached at the C-6 position interferes with the toggle switch residues, W6.48 and F3.36, and prevents the receptor from assuming an active state conformation. This prevents the G protein from inserting and therefore signaling cannot occur.

Project 2: Aminoalkylindole Pharmacophore Model

Evidence for an unidentified receptor was found in HEK 293 and T98G astrocytoma cells. This receptor binds aminoalkylindoles, but not other traditional CB ligands. This suggests that the unidentified receptor is not a CB receptor or CB-like receptor. This new receptor couples to $G_{i/o}$ G-proteins and therefore is a GPCR. A pharmacophore model for aminoalkylindoles binding to this new GPCR was developed based on the ligands that were available. The pharmacophore model determined four

aromatic groups are important for binding, along with a hydrogen bond acceptor, and a hydrophobic feature. This model can hopefully provide insights for the development of additional ligands to study this new receptor. In fact, several more AAI analogs are proposed here that should provide more information on the structural importance of key moieties found in some AAI compounds. Once more ligands have been developed and tested; a 3D-QSAR model can be generated. This would provide more details about the structural and electronic features that affect binding to this AAI receptor.

REFERENCES

1. Matsuda, L.A., et al., *Structure of a cannabinoid receptor and functional expression of the cloned cDNA.* Nature, 1990. **346**(6284): p. 561-4.
2. Herkenham, M., et al., *Cannabinoid receptor localization in brain.* Proc Natl Acad Sci U S A, 1990. **87**(5): p. 1932-6.
3. Munro, S., K.L. Thomas, and M. Abu-Shaar, *Molecular characterization of a peripheral receptor for cannabinoids.* Nature, 1993. **365**(6441): p. 61-5.
4. Benito, C., et al., *Cannabinoid CB2 receptors and fatty acid amide hydrolase are selectively overexpressed in neuritic plaque-associated glia in Alzheimer's disease brains.* J Neurosci, 2003. **23**(35): p. 11136-41.
5. Cianchi, F., et al., *Cannabinoid receptor activation induces apoptosis through tumor necrosis factor alpha-mediated ceramide de novo synthesis in colon cancer cells.* Clin Cancer Res, 2008. **14**(23): p. 7691-700.
6. Howlett, A.C., *Cannabinoid receptor signaling.* Handb Exp Pharmacol, 2005(168): p. 53-79.
7. Oldham, W.M. and H.E. Hamm, *Heterotrimeric G protein activation by G-protein-coupled receptors.* Nat Rev Mol Cell Biol, 2008. **9**(1): p. 60-71.
8. Rajagopal, S., K. Rajagopal, and R.J. Lefkowitz, *Teaching old receptors new tricks: biasing seven-transmembrane receptors.* Nat Rev Drug Discov, 2010. **9**(5): p. 373-86.
9. Palczewski, K., et al., *Crystal structure of rhodopsin: A G protein-coupled receptor.* Science, 2000. **289**(5480): p. 739-45.
10. Rasmussen, S.G., et al., *Crystal structure of the beta2 adrenergic receptor-Gs protein complex.* Nature, 2011. **477**(7366): p. 549-55.
11. Hanson, M.A., et al., *Crystal structure of a lipid G protein-coupled receptor.* Science, 2012. **335**(6070): p. 851-5.
12. Granier, S., et al., *Structure of the delta-opioid receptor bound to naltrindole.* Nature, 2012. **485**(7398): p. 400-4.
13. Manglik, A., et al., *Crystal structure of the micro-opioid receptor bound to a morphinan antagonist.* Nature, 2012. **485**(7398): p. 321-6.
14. Hurst, D.P., Singh, J., Reggio, P.H., *Structural Biology of Endocannabinoid Targets and Enzymes: Components Tuned to the Flexibility of Endogenous Ligands*, in *Endocannabinoids: Molecular, Pharmacological, Behavioral, and Clinical Features*, E. Murillo-Rodriquez, Editor. 2012, Bentham Science Publishers. p. 92-137.
15. Hurst, D.P., et al., *A lipid pathway for ligand binding is necessary for a cannabinoid G protein-coupled receptor.* J Biol Chem, 2010. **285**(23): p. 17954-64.
16. Pertwee, R.G., *Cannabinoid pharmacology: the first 66 years.* Br J Pharmacol, 2006. **147 Suppl 1**: p. S163-71.

17. Devane, W.A., et al., *Isolation and structure of a brain constituent that binds to the cannabinoid receptor.* Science, 1992. **258**(5090): p. 1946-9.
18. Mechoulam, R., et al., *Identification of an endogenous 2-monoglyceride, present in canine gut, that binds to cannabinoid receptors.* Biochem Pharmacol, 1995. **50**(1): p. 83-90.
19. Pertwee, R.G., et al., *International Union of Basic and Clinical Pharmacology. LXXIX. Cannabinoid receptors and their ligands: beyond CB(1) and CB(2).* Pharmacol Rev, 2010. **62**(4): p. 588-631.
20. Rhee, M.H., et al., *Cannabinol derivatives: binding to cannabinoid receptors and inhibition of adenylylcyclase.* J Med Chem, 1997. **40**(20): p. 3228-33.
21. Recht, L.D., et al., *Antitumor effects of ajulemic acid (CT3), a synthetic non-psychoactive cannabinoid.* Biochem Pharmacol, 2001. **62**(6): p. 755-63.
22. Iwamura, H., et al., *In vitro and in vivo pharmacological characterization of JTE-907, a novel selective ligand for cannabinoid CB2 receptor.* J Pharmacol Exp Ther, 2001. **296**(2): p. 420-5.
23. Haubrich, D.R., et al., *Pharmacology of pravadoline: a new analgesic agent.* J Pharmacol Exp Ther, 1990. **255**(2): p. 511-22.
24. Bell, M.R., et al., *Antinociceptive (aminoalkyl)indoles.* J Med Chem, 1991. **34**(3): p. 1099-110.
25. Pacheco, M., et al., *Aminoalkylindoles: actions on specific G-protein-linked receptors.* J Pharmacol Exp Ther, 1991. **257**(1): p. 170-83.
26. Howlett, A.C., et al., *Nonclassical cannabinoid analgetics inhibit adenylate cyclase: development of a cannabinoid receptor model.* Mol Pharmacol, 1988. **33**(3): p. 297-302.
27. Ward, S.J., et al., *Pravadoline: profile in isolated tissue preparations.* J Pharmacol Exp Ther, 1990. **255**(3): p. 1230-9.
28. D'Ambra, T.E., et al., *Conformationally restrained analogues of pravadoline: nanomolar potent, enantioselective, (aminoalkyl)indole agonists of the cannabinoid receptor.* J Med Chem, 1992. **35**(1): p. 124-35.
29. Kuster, J.E., et al., *Aminoalkylindole binding in rat cerebellum: selective displacement by natural and synthetic cannabinoids.* J Pharmacol Exp Ther, 1993. **264**(3): p. 1352-63.
30. Felder, C.C., et al., *Comparison of the pharmacology and signal transduction of the human cannabinoid CB1 and CB2 receptors.* Mol Pharmacol, 1995. **48**(3): p. 443-50.
31. Reggio, P.H., et al., *The bioactive conformation of aminoalkylindoles at the cannabinoid CB1 and CB2 receptors: insights gained from (E)- and (Z)-naphthylidene indenes.* J Med Chem, 1998. **41**(26): p. 5177-87.
32. Stark, S., M.A. Pacheco, and S.R. Childers, *Binding of aminoalkylindoles to noncannabinoid binding sites in NG108-15 cells.* Cell Mol Neurobiol, 1997. **17**(5): p. 483-93.
33. Kreitzer, F.R. and N. Stella, *The therapeutic potential of novel cannabinoid receptors.* Pharmacol Ther, 2009. **122**(2): p. 83-96.
34. Atwood, B.K., et al., *Expression of G protein-coupled receptors and related proteins in HEK293, AtT20, BV2, and N18 cell lines as revealed by microarray analysis.* BMC Genomics, 2011. **12**: p. 14.
35. Pizza, M., et al., *Subunit S1 of pertussis toxin: mapping of the regions essential for ADP-ribosyltransferase activity.* Proc Natl Acad Sci U S A, 1988. **85**(20): p. 7521-5.

36. Friesner, R.A., et al., *Glide: a new approach for rapid, accurate docking and scoring. 1. Method and assessment of docking accuracy.* J Med Chem, 2004. **47**(7): p. 1739-49.
37. Halgren, T.A., et al., *Glide: a new approach for rapid, accurate docking and scoring. 2. Enrichment factors in database screening.* J Med Chem, 2004. **47**(7): p. 1750-9.
38. Rhee, M.H., *Functional role of serine residues of transmembrane dopamin VII in signal transduction of CB2 cannabinoid receptor.* J Vet Sci, 2002. **3**(3): p. 185-91.
39. Dixon, S.L., et al., *PHASE: a new engine for pharmacophore perception, 3D QSAR model development, and 3D database screening: 1. Methodology and preliminary results.* J Comput Aided Mol Des, 2006. **20**(10-11): p. 647-71.
40. Manera, C., et al., *Rational design, synthesis, and pharmacological properties of new 1,8-naphthyridin-2(1H)-on-3-carboxamide derivatives as highly selective cannabinoid-2 receptor agonists.* J Med Chem, 2009. **52**(12): p. 3644-51.

APPENDIX A

PHARMACOPHORE MODEL MEASUREMENTS

Table 3. Distances between the features in the Pharmacophore Model

Site1	Site2	Distance (Å)
A3	H6	2.925
A3	R7	3.418
A3	R8	5.086
A3	R9	4.082
A3	R10	3.647
H6	R7	2.67
H6	R8	4.815
H6	R9	6.901
H6	R10	5.923
R7	R8	2.153
R7	R9	6.183
R7	R10	4.858
R8	R9	6.632
R8	R10	5.215
R9	R10	2.443

Table 4. Angles between the features in the Pharmacophore Model

Site1	Site2	Site3	Angle (°)
H6	A3	R7	49
H6	A3	R8	67.8
H6	A3	R9	159.7
H6	A3	R10	128.3
R7	A3	R8	18.8
R7	A3	R9	110.7
R7	A3	R10	86.8
R8	A3	R9	92
R8	A3	R10	71.2
R9	A3	R10	36.3
A3	H6	R7	75.1

A3	H6	R8	78
A3	H6	R9	11.8
A3	H6	R10	28.9
R7	H6	R8	3
R7	H6	R9	63.3
R7	H6	R10	54
R8	H6	R9	66.2
R8	H6	R10	57
R9	H6	R10	20.2
A3	R7	H6	55.8
A3	R7	R8	130.5
A3	R7	R9	38.1
A3	R7	R10	48.6
H6	R7	R8	173.2
H6	R7	R9	94
H6	R7	R10	99.7
R8	R7	R9	92.4
R8	R7	R10	87.1
R9	R7	R10	21.6
A3	R8	H6	34.2
A3	R8	R7	30.7
A3	R8	R9	38
A3	R8	R10	41.4
H6	R8	R7	3.8
H6	R8	R9	72.2
H6	R8	R10	72.3
R7	R8	R9	68.6
R7	R8	R10	68.5
R9	R8	R10	19.5
A3	R9	H6	8.5
A3	R9	R7	31.1
A3	R9	R8	50
A3	R9	R10	62.1
H6	R9	R7	22.7
H6	R9	R8	41.6
H6	R9	R10	56.7
R7	R9	R8	18.9

R7	R9	R10	47
R8	R9	R10	45.4
A3	R10	H6	22.8
A3	R10	R7	44.6
A3	R10	R8	67.4
A3	R10	R9	81.6
H6	R10	R7	26.4
H6	R10	R8	50.7
H6	R10	R9	103.1
R7	R10	R8	24.4
R7	R10	R9	111.4
R8	R10	R9	115.2

APPENDIX B

TABLES OF COMPOUNDS

Table 5. The compounds developed by Manera et al. with binding/activity data

Compounds	CB2 Binding Assay (nM) Ki IC50	β-Arrestin 2 EC50/IC50 (nM)	cAMP EC50/IC50 (nM)
A1 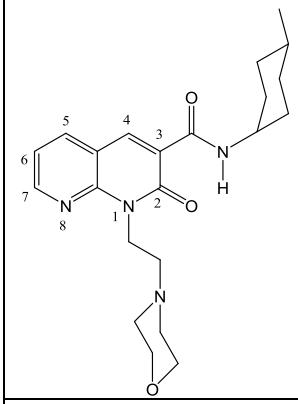	1.90 2.89	17.53	28.0
A2 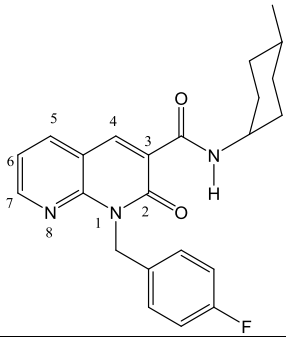	0.90 1.37	29.54	29.59
5 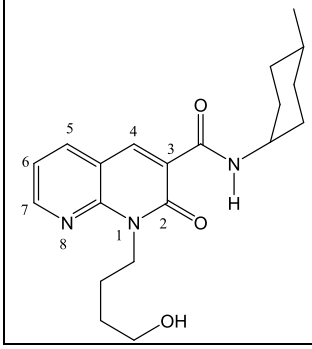	53.34 210.17	23.70	NA

Compounds	CB2 Binding Assay (nM) Ki IC50	β-Arrestin 2 EC50/IC50 (nM)	cAMP EC50/IC50 (nM)
17 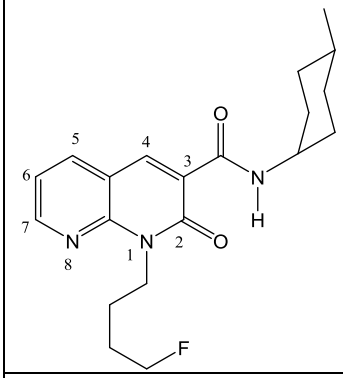	1.36 5.35	21.83	20.58
20 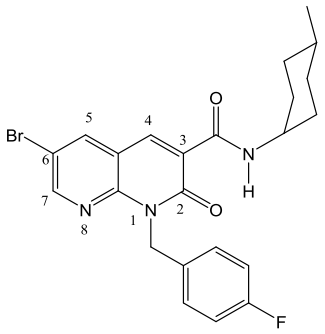	0.18 0.72	31.59	NA
21 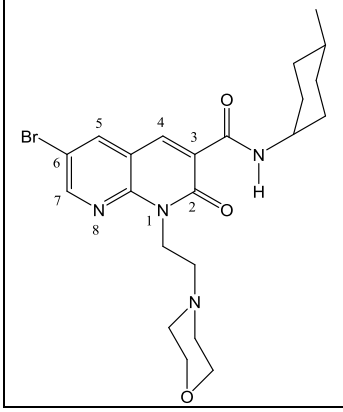	1.26 4.95	32.12	59.54

Compounds	CB2 Binding Assay (nM) Ki IC50	β-Arrestin 2 EC50/IC50 (nM)	cAMP EC50/IC50 (nM)
26 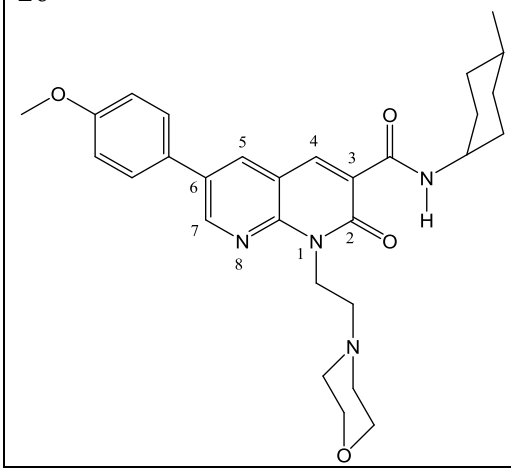	1.47 5.56	54.0	NA

Table 6. Aminoalkylindoles used to develop pharmacophore model and their binding affinities

Compound	Binding Affinity (Ki)
WIN55212-2 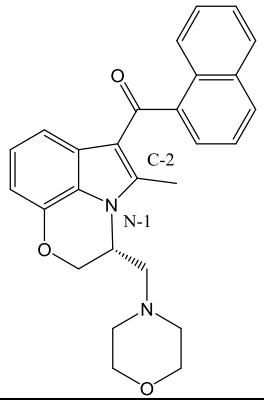	Biphasic displacement curve 0.027 nM (0.0004 to 0.027) 72 nM (54 to 8000)
TK-18 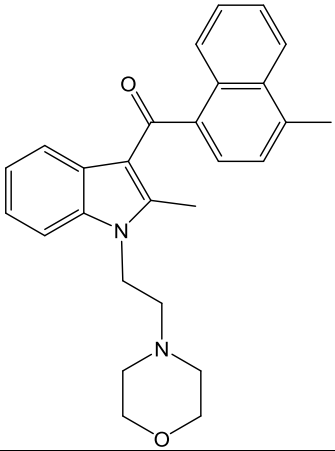	Biphasic Displacement Curve 0.8 nM (0.39 to 1.5) 90 nM (61 to 130)
CBX-002 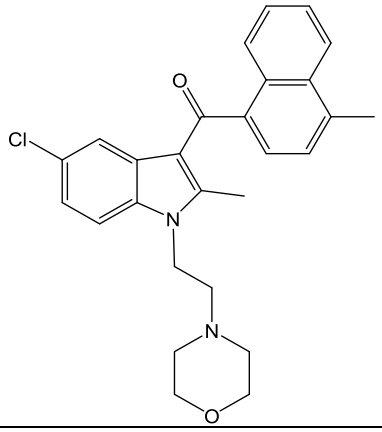	Biphasic Displacement Curve 10 nM (1.1 to 19) 2300 nM (130 to 1800)

Compound	Binding Affinity (Ki)
CBX-003 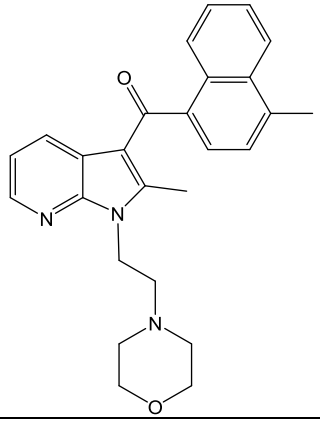	Biphasic Displacement Curve 0.4 nM (0.12 to 0.43) 382 nM (120 to 1300)
CBX-004 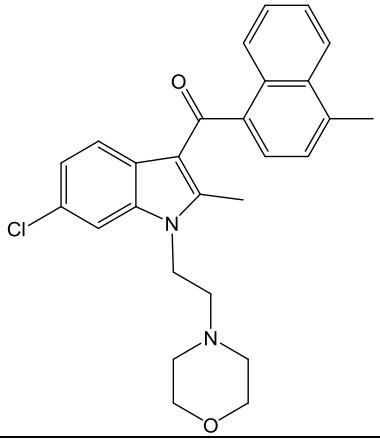	3.5 nM (1.0 to 12)
CBX-005 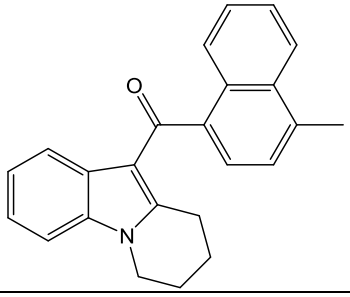	Biphasic Displacement Curve 5.5 nM (0.15 to 200) 2600 nM (16 to 41000)

Compound	Binding Affinity (Ki)
CBX-006 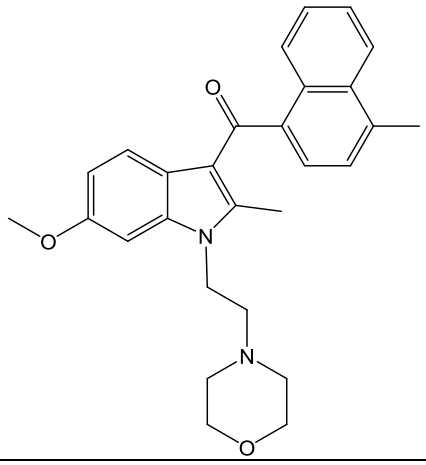	113 nM (50 to 250)
CBX-008 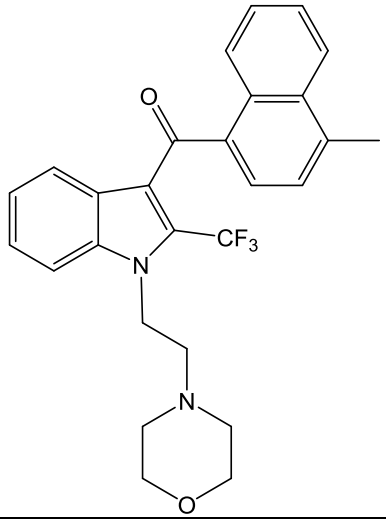	972 nM (410 to 2300)
CBX-009 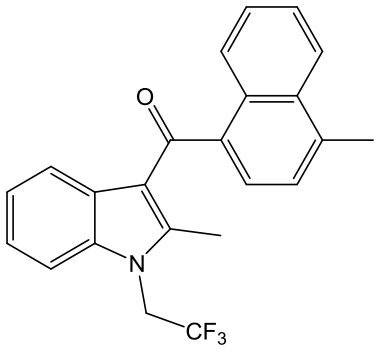	1.8 nM (0.41 to 7.6)

Compound	Binding Affinity (Ki)
CBX-010 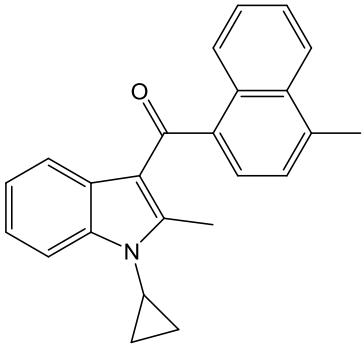	118 nM (61 to 230)
CBX-011 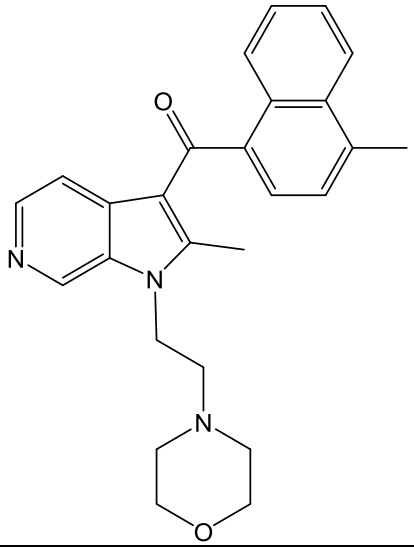	Biphasic Displacement Curve 5.8 nM (0.25 to 5.8) 21000 nM (210 to 22000)
JHW-015 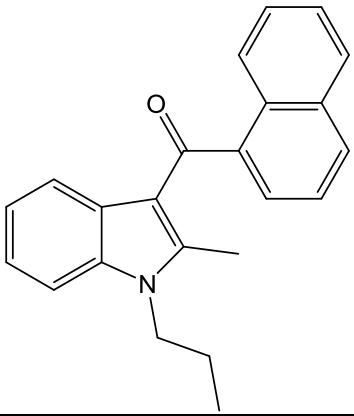	41 nM (31 to 54)

Compound	Binding Affinity (Ki)
JWH-120 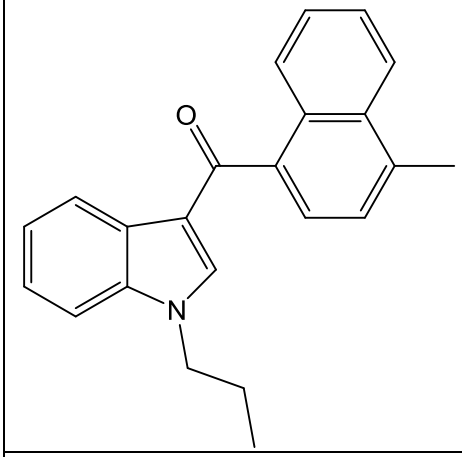	319 nM (120 to 850)
JWH-148 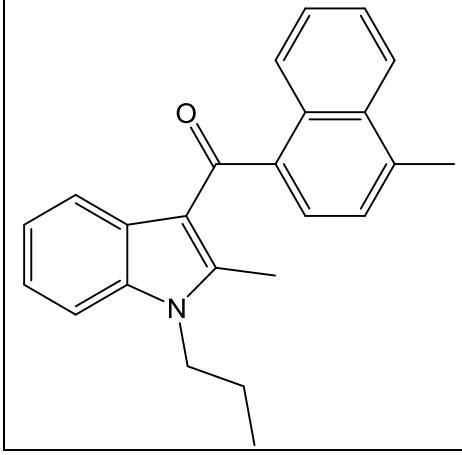	95 nM (49 to 180)

Compound	Binding Affinity (Ki)
Z Hydrogen Indene 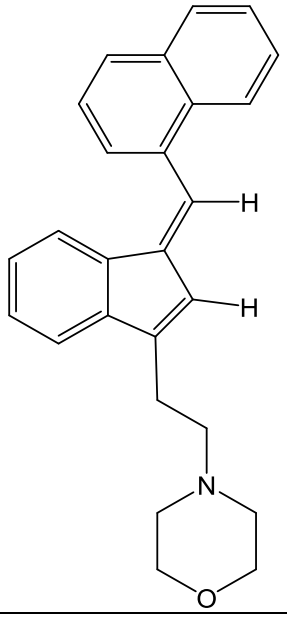	437 nM
Z Methyl Indene 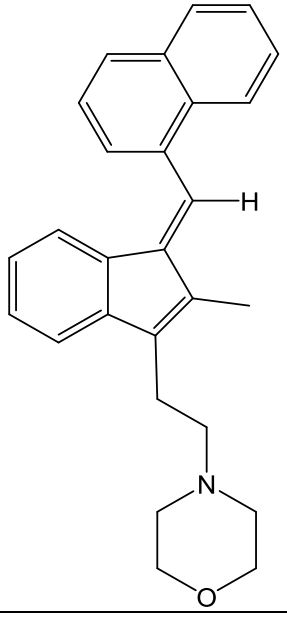	466 nM

Compound	Binding Affinity (Ki)
E Hydrogen Indene 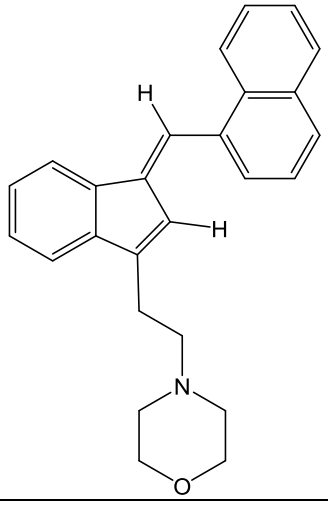	3400 nM
E Methyl Indene 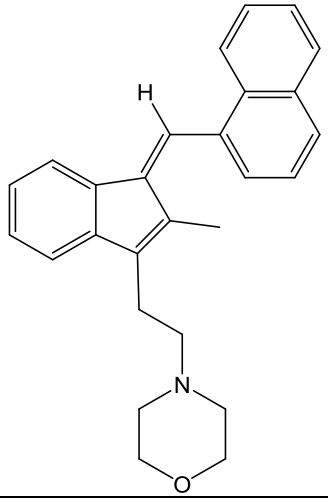	NA